LA-UR-12-20389
Approved for public release; distribution is unlimited.

Title:	Stopped Pion Absorption by Complex Nuclei
Author(s):	Iljinov, Alexander S Cherepanov, Evgeny A Chigrinov, Sergey E Mashnik, Stepan G
Intended for:	MCNP6 refrences package

Stopped Pion Absorption by Complex Nuclei

A. S. Iljinov[1], E. A. Cherepanov[2],

S. E. Chigrinov[3], S. G. Mashnik [2,*]

[1]*Institute for Nuclear Research, Academy of Science of the USSR*

[2]*Joint Institute for Nuclear Research, Dubna, Moscow Region, USSR*

[3]*Institute for Nuclear Engineering of the BSSR Academy of Science, Minsk*

Abstract

New experimental data on stopped negative pion absorption by complex nuclei (energy spectra and angular correlations of secondary particles, isotope yield, fission probability, angular momentum of residual nuclei) are analysed within the framework of the earlier model suggested by the authors /1/. Comparison is made with other up-to-date models of the process. The contributions of different pion-absorption mechanisms are considered.

We reproduce here this 1980 INR Report as it was never published in a journal but represents a historical interest of using the Modified Exciton Model (MEM) to account for preequilibrium processes in stopped pion absorption by nuclei. MEM was later incorporated in the Cascade-Exciton Model (CEM), and was and still is used in dozens of countries all over the world. E.g., the current CEM03.03 and LAQGSM03.03 event-generators of the latest LANL Monte Carlo transport code MCNP6 have today modified parts from the FORTRAN code of that old version of MEM/CEM.

---

[*]Current and permanent address: XCP-3, Computational Physics Division, Los Alamos National Laboratory, Los Alamos, NM 87545, USA

ACADEMY OF SCIENCES OF THE USSR
INSTITUTE FOR NUCLEAR RESEARCH

A. S. Iljinov, E. A. Cherepanov*,
S. E. Chigrinov**, S. G. Mashnik*

Stopped Pion Absorption by Complex Nuclei

* Joint Institute for Nuclear Research, Dubna.

** Institute for Nuclear Engineering of the BSSR Academy of Sciences, Minsk.

P-0156

MOSCOW
1980

УДК 539. 172. 5

New experimental data on stopped negative pion absorption by complex nuclei (energy spectra and angular correlations of secondary particles, isotope yield, fission probability, angular momentum of residual nuclei) are analysed within the framework of the earlier model suggested by the authors /1/. Comparison is made with other up-to-date models of the process. The contributions of different pion-absorption mechanisms are considered.

Рукопись поступила в издательский отдел ИЯИ АН СССР 30.04. 1980г.

Редактор Ю. Г. Балашко
Технический редактор Н. Л. Нольде
Корректор А. С. Ильинов

Т-00857 от 28.05.1980г. Заказ № 5038
Ф-т 60 x 84/8 Уч.-изд.л. 2,9 Тираж 150 экз.

Отпечатано на ротапринте методом прямого репродуцирования с оригинала, представленного авторами.

Издательский отдел Института ядерных исследований АН СССР. 113152, Москва, Загородное шоссе, д. 10, корп.9.

1. Introduction

Stopped negative pion absorption in atomic nuclei occupies a special place in modern physics due to intimate interweaning of various problems of mesoatomic physics, pion-nucleus interaction, nuclear reactions and nuclear structure. The study of this phenomenon was started about three decades ago, just as pion beams were obtained. Since that vast experimental information has been accumulated and a lot of theoretical works performed that allow understanding of the main features of the process. The progress has been most appreciable for some recent years upon putting in operation of "meson factories" in the USA, Switzerland, Canada and creation of new intensive pion beams in JINR and CERN. A considerable portion of experimental and theoretical researches dealt with the study of the mechanism of π^--absorption in light nuclei. However more complicated but not less important reactions on medium-weight and heavy nuclei were studied in less detail. Some years ago, when no results of experiments on meson factories were available, we suggested a model to describe stopped π^--meson absorption in medium-weight and heavy nuclei /1/.

The aim of the present work is to analyse new experimental data within the framework of the model developed and to compare it with later models /2,3/ of pion absorption.

2. The Main Principles of Absorption and Ways of Its Description

2.1. Formation and De-excitation of a Pionic Atom

Up-to-date models consider the absorption of negative pions by a nucleus to be a multistage process. At the first stage, the π^--meson stopped in the matter is captured by the Coulomb field of the nucleus thus forming a highly excited pionic atom. De-excitation of the atom, i.e. transitions of the pion to lower orbits involving emission of Auger-electrons and x-rays, is terminated upon pion absorption by nucleus from one of the pionic orbits.

The understanding of the process as a whole requires the knowledge of the radial dependence of the pion absorption probability $P_{abs}(r)$. For the probability of pion absorption from the state with the principal and orbital quantum numbers n and l prescribed, we have

$$P_{n,\ell}(r) \sim r^2 \rho(r) \left| \Psi_{n,\ell}(r) \right|^2 \qquad (1)$$

where $\rho(r)$ is the nuclear density; $\Psi_{n,\ell}(r)$ is the pion wave function. Expression (1) needs summation over all of the mesoatomic states in accordance with their populations specified by the level width $\Gamma_{n,\ell}$ and initial distribution over n and l of the pions captured by the Coulomb field of the nucleus.

The shape of the function $P_{abs}(r)$ may be obtained without calculating the population of mesoatomic states, by analysing both the experimental data on x-ray transitions in pionic atoms /4/ and the calculated /5/ wave functions $\Psi_{n,\ell}(r)$. Based on the analysis such as this the authors of /1/ have supposed that for medium-weight and heavy nuclei pion absorption takes place in the surface layer of the nucleus. As a first approximation, the probability density of pion absorption in the nucleus is taken in the form

$$P_{abs}(r) \sim \exp\left\{-[r-(c+\Delta r)]^2/2\sigma^2\right\} \qquad (2)$$

where $\sigma = 1.3 \cdot 10^{-13}$ cm, and c is the parameter in the nuclear density distribution

$$\rho(r) = \rho_0 \left\{1 + \exp\left[(r-c)/a\right]\right\}^{-1}. \qquad (3)$$

The values of the parameters in expression (3) are taken from the experiments on electron scattering by nuclei as $a = 0.545 \cdot 10^{-13}$ cm and $c = 1.07\, A^{1/3} \cdot 10^{-13}$ cm. The value of the parameter $\Delta r \geqslant 0$ specifies the displacement of the maximum of the Gaussian curve $P_{abs}(r)$ relative to the half-radius of nuclear density. In /1/ the quantity Δr was found from the condition of the best fit to the experimental data on pion absorption in nuclei.

Recently in /3/ a consistent calculation of pion absorption probability has been performed starting from the formation of a pionic atom and ceasing with its de-excitation. The earlier assumption /1/ on a surface nature of pionic absorption has been verified. Fig. 1 shows the parameter $\Delta r = 0$, while the Gaussian curve width has a lower value than in /1/ $\sigma = 0.78 \cdot 10^{-13}$ cm.*

---

* In the present work the parameters $\Delta r = 0$ and $\sigma = 1.3 \cdot 10^{-13}$ cm will be used in calculations.

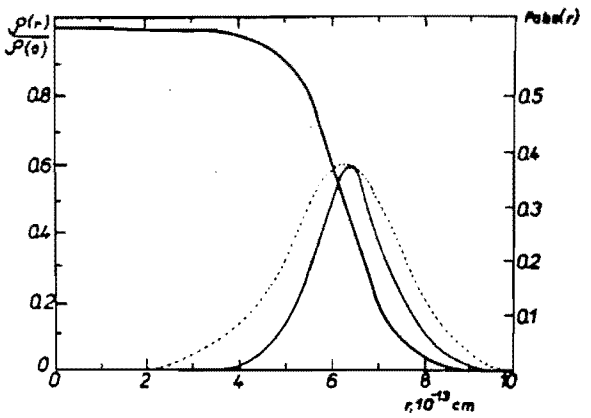

Fig. 1. Distribution of the density of nuclear matter $\rho(r)/\rho_0$ (left-hand scale) and absorption probability $P_{abs}(r)$ (right-hand scale) for ^{181}Ta nucleus. Thick solid curve, calculation for $\rho(r)/\rho_0$ by formula (3); thin solid curve, calculation for $P_{abs}(r)$ from [3]; dotted curve, calculation for $P_{abs}(r)$ by formula (2) with $\Delta r = 0$ (2) (in relative units).

It is worth noting that the function $P_{abs}(r)$ does not practically change with wide-range variation of the initial distribution over for pions captured by the Coulomb potential of the nucleus. In other words, the effects of valent electrons and other minute details on pion - atomic electron shell interaction at the initial stage of pion transition from a continuous spectrum into a discrete one that were ignored in /3/ cannot alter the conclusion that pion absorption occurs in the surface layer of the nucleus.

An important aspect, i.e. surface nature of pion absorption, is taken into account by the models suggested in /1,3/.

2.2. Pion Absorption in the Nucleus

Since the law of energy-momentum conservation forbids the absorption of pion by a free nucleon, this process will be strongly suppressed on the intranuclear nucleon as well. A pion is therefore absorbed by nuclear substructures such as multinucleonic associations. It is generally accepted that a pion is absorbed by a simplest two-nucleon association. For the first time an absorption mechanism such as that was suggested in /6/ dealing with pion absorption by (n,p) or (p,p) pairs

$$\pi^- + (np) \rightarrow n + n \qquad (4a)$$

$$\pi^- + (pp) \rightarrow p + n \qquad (4b)$$

In the simplest case, neglecting spin effects, charge state of two nucleons is specified by the number of pairs of a given type and then the probability of absorption on the n-p pair is equal to

$$w_{np} = \frac{NZ}{NZ + Z(Z-1)/2} \qquad (5)$$

where N and Z are numbers of neutrons and protons, respectively, in the nucleus. Expression (5) implies that in this case pion is absorbed more often by n-p rather than by p-p pairs:

$$R \equiv w_{np} / w_{pp} = 2N/(Z-1) > 1. \qquad (6)$$

It should be noted that allowance for spin effects may appreciably change the value of the ratio R. Different theoretical estimations of this quantity lay within $0 < R < 10$ (see, for example, the analysis of the isospin effect on R in [3]). For the time being neither experimental data allow the value of R to be fixed, since the measured ratio R_e^* for the number of outgoing n-n pairs to the number of p-p pairs has significant uncertainties and may range from 1.5 to 5 [7].

Because of the uncertainties mentioned the quantity R must be considered as a parameter whose value is found through the comparison with the experiment. The calculations in this work as well as in [5] were performed using formula (5); in ref. [2] $R = 4$.

After the absorption, the pion mass m_π has the form of kinetic energy of secondary nucleons, each having the energy $E = m_\pi/2$ in the centre of mass system. In the c.m.s. secondary nucleons fly apart isotropically in opposite directions. In the laboratory system, the energy of secondaries will have certain deviation about the quantity $m_\pi/2$ due to the momentum of intranuclear nucleons. The models [1-3] allow for "smearing" over "quasideuteron"** momenta in the nucleus: a quasideuteron momentum is equal to the sum of the momenta of two intranuclear nucleons determined from the appropriate Fermi-distribution.

2.3. Rescattering and Absorption of Fast Nucleons, the Products of Pion Capture, in the Nucleus

Thus, pion absorption in the diffuse layer of the nucleus results in two nucleons with energy 50 ÷ 100 MeV. Depending on their directions and the point at which pion is absorbed, nucleons may escape from the nucleus either without interaction or undergoing one or several collisions with intranuclear nucleons. This stage is similar

---

* $R_e \leq R$ because the nucleon emitted from the nucleus may undergo rescattering with charge exchange.

** In what follows the term "two-nucleon association" is replaced by "quasideuteron" though these words do not have quite the same meaning.

to ordinary nuclear reaction when an intermediate energy nucleon incident on the nucleus initiate intranuclear cascade in it.

To describe those processes in /1,3/ the model of intranuclear cascades is used that works rather well when 100 MeV nucleons impinge on nuclei (see, for example, review /8/). It should be noted, that no additional parameters are introduced as all the parameters of the cascade model are determined independently from the analysis of nucleon-nucleus interactions. Detailed description of the intranuclear cascade model may be found in review /8/. Therefore, only its basic assumptions will be considered here. In this model the nucleon-nucleus interaction is reduced to a series of successive nucleon-nucleon collisions. The nucleus is considered as a degenerate Fermi-gas of free nucleons enclosed in a spherical potential well. Density distribution for intranuclear nucleons is taken in the form of (3).

In ref. /2/ two "parallel" intranuclear cascades are described in terms of the exciton model (see review /9/). One of the difficulties involved in calculation of ordinary nuclear reactions is to choose the initial configuration of the system, i.e. the number of particles p and holes h. Eventually, it is varied to achieve best agreement with experiment. As the initial configuration for each of the cascades, the authors of /2/ applied 1p-1h with the energy of 70 MeV. The subsequent competition of different modes of decay of an intermediate system in a cascade process is specified by partial width for particle emission and exciton-exciton interaction, whose calculation details are given in review /10/.

3.4. Establishment of Statistical Equilibrium in the Residual Nucleus

Following the intranuclear cascade, "holes" are formed in degenerate Fermi-gas due to collisions between cascade particles and intranuclear nucleons. Besides, some of the cascade nucleons cannot overcome nuclear potential and will be in a bound states above Fermi energy. Since the system formed is nonequilibrium, particle emission from the residual nucleus is possible before the "evaporative" stage of the process.

To estimate the role of pre-equilibrium emission of particles from a residual nucleus, one may use the exiton model /9/, for which the initial state will be given by the preceeding stage of rescattering of fast neutrons. In the present study of equilibration stage is described more successively than in /1/.

The condition specifying the termination of the fast cascade stage is important for the model. To this end, a standard model includes the

cutoff energy E_{cut} below which particles are considered to be absorbed by the nucleus [8]. A sharp cutoff such as that causes irregularities in a number of reaction characteristics in the vicinity of this point, for example in the energy spectra of the secondaries [11]. In [11] it is suggested to use another criterion according to which a secondary particle is considered as a cascade one, namely the proximity of an imaginary part of the optical potential $W_{opt.mod.}(r)$ calculated in the cascade model to the appropriate experimental value $W_{opt.exp.}(r)$. This value is characterized by the parameter

$$P = \frac{W_{opt.mod.} - W_{opt.exp.}}{W_{opt.exp.}} . \qquad (7)$$

The modified intranuclear cascade model better describes inelastic interactions of 30-100 meV protons with nuclei [12]. In what follows, the value P = 0.3 is used extracted from the analysis of the experimental proton-nucleus data [12].

The effect of pre-equilibrium particle emission on some integral characteristics of pion absorption in nuclei (for example, mean multiplicity and energy spectra of emitted nucleons, isotope yield) is insignificant and can be ignored in the first approximation in models [1,3]. As a rule, in the present paper experimental data are compared to calculations performed with neglect of pre-equilibrium emission. However, in some details of the phenomenon pre-equilibrium processes may show themselves rather distinctly, and for this case the calculations will be given allowing for particle emission at the stage of establishing of the thermodynamic equilibrium in an excited nucleus.

As to the model [2], it implies the equilibration stage because of the exciton formalism chosen to describe the nuclear reaction.

2.5. Particle Emission and Fission of an Excited "Compound" Nucleus

Once thermodynamic equilibrium has been established, a highly excited residual nucleus either gradually "evaporates" particles or undergoes fission. De-excitation and fission of the residual nucleus proceed in the same way as in an ordinary compound nucleus formed in reactions with low-energy particles or heavy ions*. In describing such a process, the statistical theory is used developed by Weisskopf [13] for particle emission and by Bohr and Willer [14], for fission.

* Here compound nucleus is the one with established thermodynamic equilibrium.

In [1-3] particular calculations of the de-excitation of compound nuclei are performed by the method developed by Dostrovsky et al [15,16]. The use is made of the level density function for the model of noninteracting particles (Fermi-gas model):

$$\rho(E^*) \sim \exp\left(2\sqrt{aAE^*}\right) \qquad (8)$$

where $a = 0.1\,\mathrm{MeV}^{-1}$ is the parameter of level density, A=Z+N. The calculations allowed for possible emission of the particles of 6 types: n, p, d, t, ^{3}He and α. The method of Dostrovsky et al. [15,16] has been extended to fission in ref. [17].

Thus, stopped pion absorption is complicated and versatile process combining in itself the features of both low-energy nuclear reactions and those initiated with intermediate-energy particles. This is exactly why the Monte-Carlo method is preferred for calculations in [1-3]. It is noteworthy that despite bulky computations, this method makes it possible to obtain, within the framework of one approach, the most consistent and detailed description of various process characteristics connected both with emission of secondaries formed following pion absorption by a multinucleon association and with the properties of an excited residual nucleus.

Before we start the analysis of the experimental data, lets summarise different theoretical approaches available. One of them [1,3] is based on the model of intranuclear cascades, another [2], on the exciton model. For the time being the former possesses great potentialities, since in contrast to the exciton method this approach allows calculation of the characteristics which exhibit most distinctly the surface character of pion absorption by the nucleus. These are, for example, high spin of residual nuclei and different correlations of emitting high-energy particles.

3. Analysis of Experimental Data

3.1. Energy Spectra of Neutrons

Neutron emission following pion absorption is an important type of the decay of highly excited nucleus. Most detailed and persistent measurements of the energy spectra of neutrons are performed in [18-21]. As an example, in Fig. 2 the results [21] are shown for the neutron spectra formed after π^--absorption in ^{59}Co and ^{197}Au targets. The spectrum has a specific feature attributed to the existence of cascade and evaporative stages of π^-- absorption. Two components, "evaporative" and fast

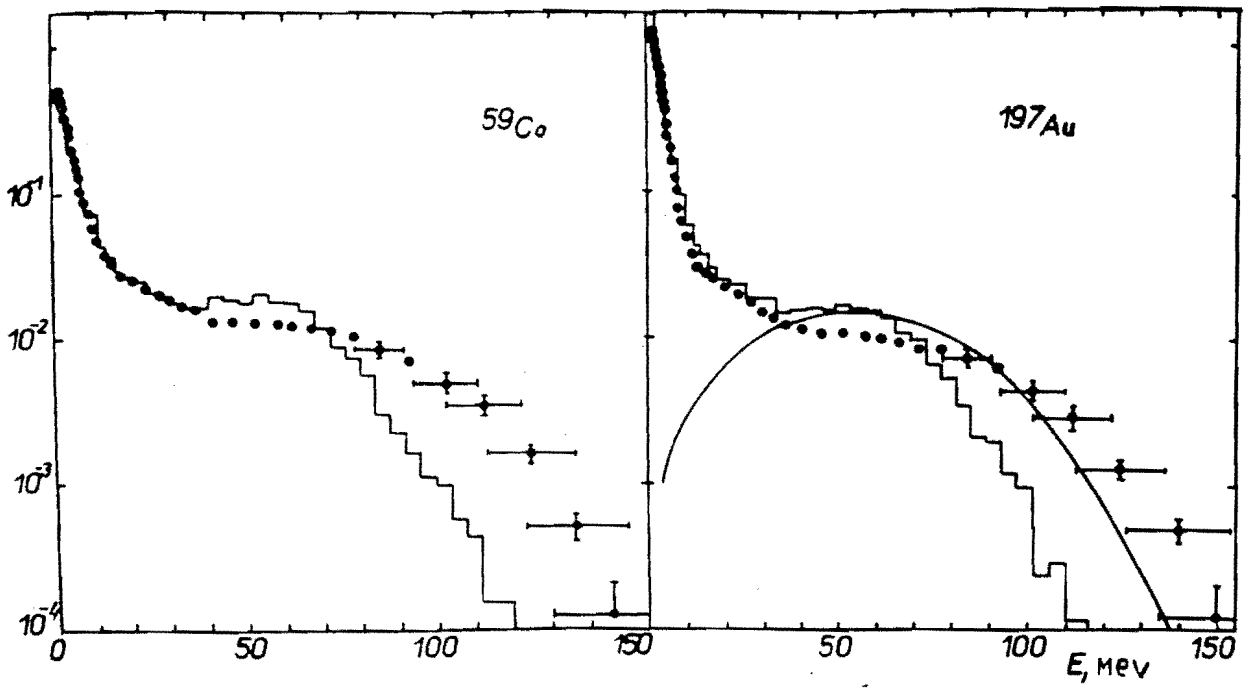

Fig. 2.
Energy spectra for neutrons (in N/π^-. Mev units) following slow negative pion absorption in ^{59}Co and ^{197}Au nuclei. Points, experimental data of [21]; histograms present authors calculation; solid curve, calculation from [22].

neutrons, are distinct in the spectrum. The evaporative part of the spectrum includes neutrons emitted by excited residual nuclei, while the high-energy spectrum is composed mainly of fast cascade particles emitted from the surface layer of the nucleus without collisions with intranuclear nucleons.

The surface character of absorption results in weak dependence of high-energy portion of the spectrum on the atomic number of the nucleus-target. Thus, mean multiplicity of fast neutrons for ^{59}Co and ^{197}Au nuclei is 1,38 and 1.32 neutrons per absorbed pion /21/. The increasing total multiplicity from 4.04 neutrons for ^{59}Co nucleus to 6.31 neutrons for ^{197}Au nucleus indicates the dependence of the evaporated neutron multiplicity on the nuclear mass results from increasing excitation energy of residual nuclei.

Theory fairly describes the evaporation part of the spectrum. At the same time, the fast component proves to be much softer than the experimental one. Though its maximum is situated at the energy $m_\pi/2 - B_n \simeq 60$ MeV (B_n is the nucleon binding energy), its "smearing" to the high-energy region seems to be insufficient. This presumably points to insufficiently correct description of high momentum component of nucleon distribution in nucleus /1,3/. The local density approximation used in these studies gives small momenta of nucleons of the nuc-

leus at its periphery and, hence, insignificant "smearing" of the neutron spectrum.

This may be proved by a simplified calculation of the fast component in the neutron spectrum [22] made on the assumption that one of the neutrons formed in reaction (4a) goes out of the nucleus without interaction, while the other is absorbed by it. Momentum distribution of intranuclear nucleons in the form

$$f(p) \sim \exp(-p^2/\alpha^2) \qquad (9)$$

where the value 13 MeV $\leq \alpha^2/2M_n \leq$ 20 MeV (M_n is nucleon mass) allows better description of the high-energy part of the spectrum of secondary particles. The remaining discrepancy for 110 MeV $\leq E_n \leq$ 140 MeV may presumably be explained by the contribution of other mechanisms of pion absorption, single-nucleonic mechanism among them.

3.2. Energy Spectra of Charged Particles

Energy spectra of charged particles emitted after absorption of stopped pions in different nuclei were measured in [23-29]. In Figs. 3 and 4 experimental spectra of protons, deuterons, tritium, helium-3 and α -particles from [27,29] are presented.

The above remarks concerning neutron spectra hold also for proton spectra. Only the evaporation component of the proton spectrum for heavy nuclei is poorly distinct due to the effect of the Coulomb barrier. The fast component of the proton spectrum is formed to reaction (4b), therefore for the energies above $E \geq 70$ MeV, as is the case of neutrons, the calculation yields more soft spectrum because of insignificant "smearing" over the momenta of intranuclear nucleons. Fig. 3 also shows the proton spectrum calculated within the framework of the exciton model [2]. The spectrum is taken from later work [27]. To eliminate the discrepancy with experiment for $E > 60$ MeV, the authors have to allow for the "smearing" over the Fermi momenta of intranuclear nucleons [30].

Of great interest is the measurement of spectra of charged complex particles, as it is a common practice to consider that such particles may be formed due to pion absorption in a more complicated, in contrast to two-nucleon, association. But before studying this problem for complex nuclei, we must elucidate the contribution of other possible mechanisms to the formation of those particles.

Evaporation is the simplest among those mechanisms. In this case a charged particle is emitted by a highly-excited nucleus at the last stage of the process. The calculations [31] have shown that none of the spectra of Fig. 3 and 4 can be obtained in this case either in shape or in absolute value.

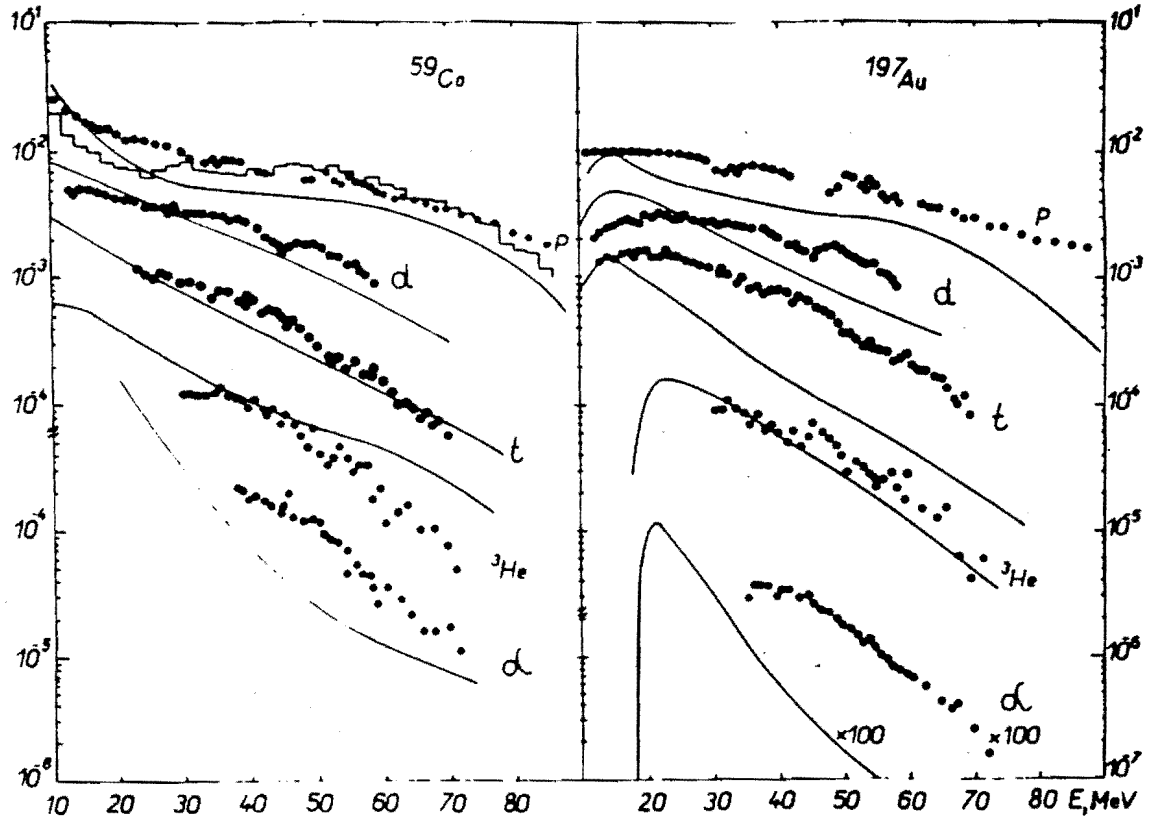

Fig. 3.
Energy spectra of p, d, t, ^{3}He and ^{4}He (in N/π^-. Mev units) emitted by ^{59}Co and ^{197}Au nuclei following slow pion absorption. Points, experimental data of [27]; solid curves, calculation results of [31]; histogram, results of calculation by the exciton model (Gadioli et al. [27]).

It is shown in /31/ that pre-equilibrium processes make an important contribution to the spectra of complex charged particles. With no assumption on the existence of complex particle-clusters prepared in the nucleus a priori, the emission rate for a pre-equilibrium particle of type B with energy ε from the nucleus with the excitation energy E^* and the number of particles and holes n=p+h will be written as /32/:

$$W_B(p,h,E^*,\varepsilon)\,d\varepsilon = \left[\gamma_B R_B(p)\,\frac{\omega(p-p_B,h,E^*-B_B-\varepsilon)}{\omega(p,h,E^*)}\times\right.$$
$$\left.\times\,\omega(p_B,0,B_B+\varepsilon)\right]\frac{(2S_B+1)}{\pi^2\hbar^3}\,\frac{m_B\,\varepsilon\,\sigma_{inv}}{g_B}\,d\varepsilon\,. \qquad (10)$$

Here S_B, m_B, B_B and σ_{inv} are spin, mass, binding energy and cross-section of inverse reaction for an emitted particle, respectively; ω is the density of particle-hole states; g_B is the density of one-particle states in the equidistant spectrum approximation. The factor $R_B(p)$ specifies a correct isotopic composition, while the pa-

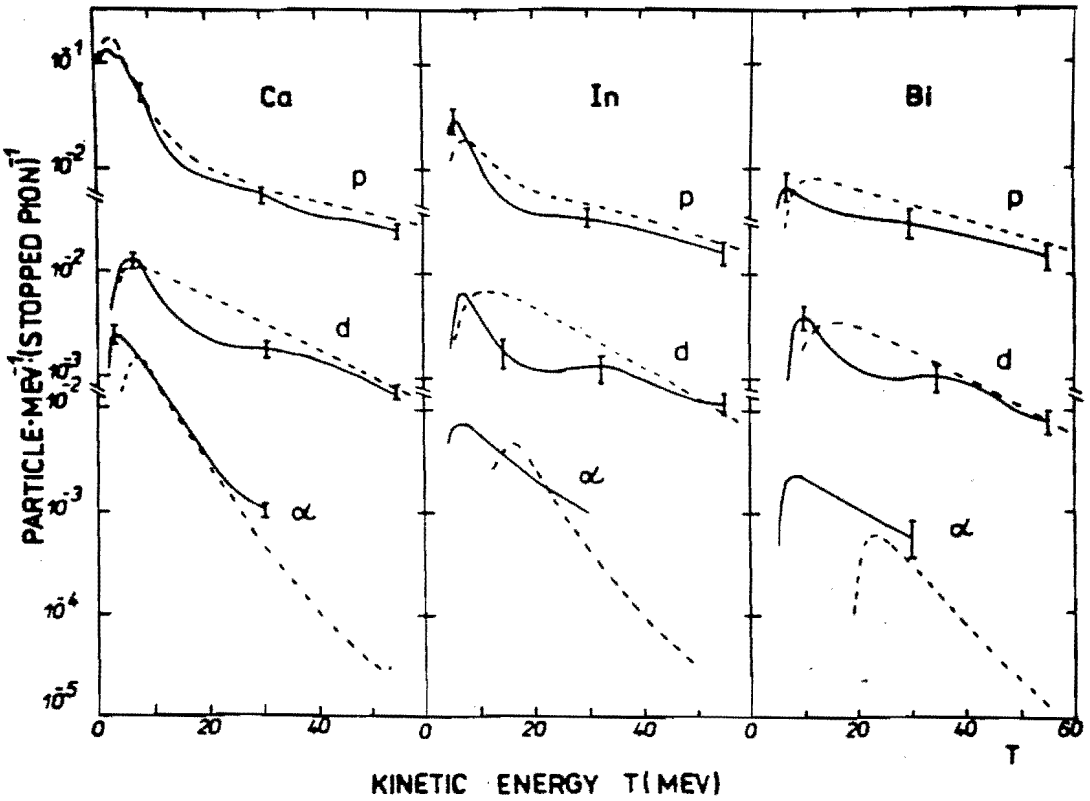

Fig. 4.
Energy spectra of protons, deuterons and α-particles (in N/π^-. Mev units) emitted by Ca, In and Bi nuclei following slow pion absorption. Solid curve, experimental results of [29]; dotted curve, calculation results.

rameter γ_B describes probability of grouping of p_B nucleons into a complex particle. If the quantity γ_B is defined as the overlapping integral for the wave functions of independent nucleons Ψ_i, and the cluster wave function Ψ_B, then the simplest estimation will give

$$\gamma_B = \left| \int \Psi_1 \dots \Psi_{p_B} \Psi_B^* \, d\vec{x}_1 \dots d\vec{x}_{p_B} \right|^2 \simeq p_B^3 \, (p_B/A)^{p_B - 1}. \qquad (11)$$

As seen from Figs. 3 and 4, the contribution of pre-equilibrium particles to spectra is large. At the same time, at high energies the calculated curves lie below the experimental points. It is possible that the discrepancy in this region may eliminate both the above mechanism of direct emission following pion capture on multinucleonic associations, and the mechanism of complex-particle emission at the stage of intranuclear cascade. The latter processes may involve intranuclear nucleon pickup with a fast nucleon as well as knocking-out of preliminarily prepared clusters in nucleus by fast nucleons.

It should be noted that the considered mechanisms of complex charged particle emission (pre-equilibrium emission, pickup and knockout process) must also show themselves in the case of inelastic proton--nucleus interaction with $E = m_{\pi}/2$. Therefore, to estimate the fraction of charged particles emitted following pion absorption by the multinucleon association (for example, by the α - cluster), it would be advisable to use the results of proton-nuclear experiments in the analysis. Thus, the experiments performed at proton energy E_p = 62 MeV /33/, 72 MeV /34/ and 90 MeV /35/ have shown that spectra of d,t ^{3}He and α - particles in proton-nuclear and pion-nuclear interactions have similar shape. This points to a great contribution of secondary processes to complex particle emission.

3.3. Correlation Between Emitted Particles

An important information on the mechanism of pion absorption in nuclei has been obtained from the measurements of energy and angular distributions of various particles in coincidence /21,36-43/. Angular correlations of two neutrons or neutron and proton have a sharp maximum at an angle of 180° for the carbon nucleus which becomes wider for heavier nuclei ^{59}Co and ^{197}Au (see Fig. 5). The picture such as that corresponds to a two-nucleon mechanism of pion absorption and is fairly described in the approach using the model of intranuclear cascades. The energy spectrum of one neutron in coincidence with another one /21/ has a wide maximum for the nucleus ^{12}C at 50-60 MeV, which also indicates a two-nucleon absorption mechanism. In kinematically complete experiments for (π^-, 2n) reaction on nuclei ^{9}Be, ^{10}B, ^{12}C, ^{14}C, ^{40}Ca /41-43/ it was possible not only to show the dominating role of a two-particle absorption mechanism, but also to get information concerning the state of an absorbing nucleon pair. Thus, it is shown in /42/ that pion is mainly absorbed in a pair of nucleons being in the 1s-state relatively each other.

3.4. Isotope Yield

This is an important characteristic of pion absorption in nuclei, dealt with in many experimental studies /3,30,40,44-59/.

The experimental data obtained show that pion absorption is accompanied with strong nuclear spallation. Thus, in the case of medium or heavy nucleus the number of emitted nucleons may achieve 15-17 /3,30, 47,50,58/, which corresponds to the excitation energy close to the pion mass. Here, multiplicity distribution is wide and ranges from 2 to $\sim$16 particles. This distribution can be easily explained by the models /1,3/. Indeed, since the energy of cascade particles ranges widely (Fig.

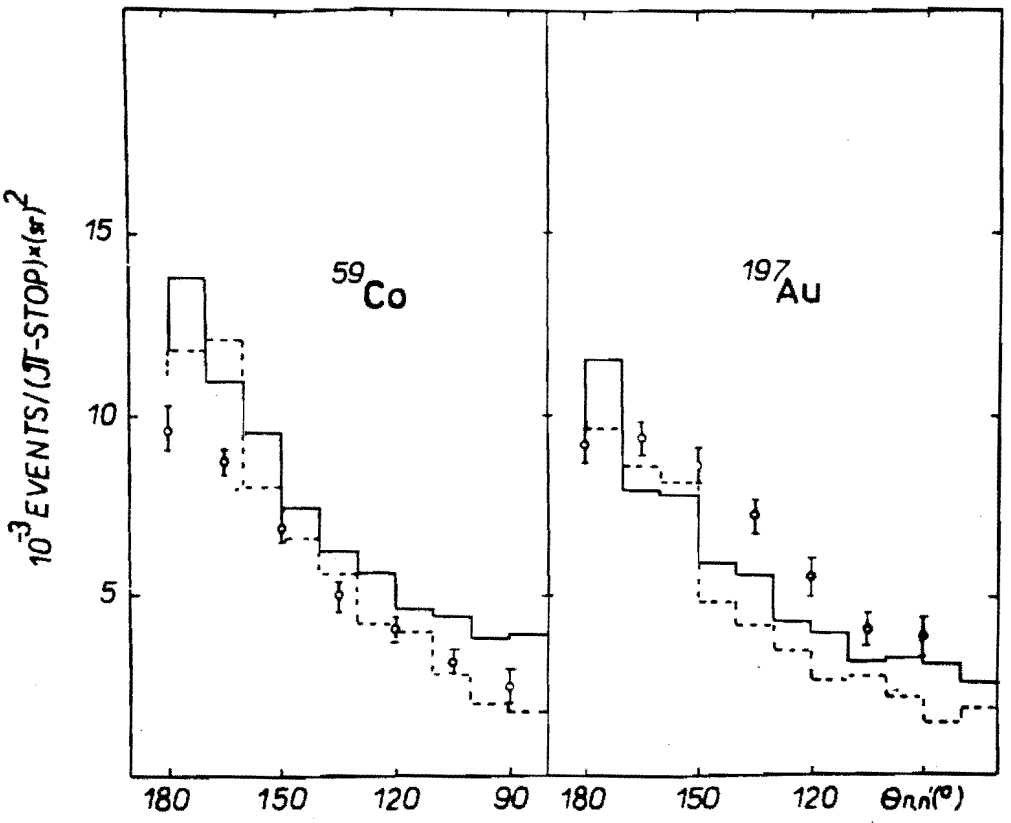

Fig. 5.
Angular correlation of two neutrons detected in coincidence following π^--absorption by ^{59}Co and ^{197}Au nuclei (neutron detection threshold E_n = 20 MeV). Histogram, calculation results; points, experimental data of [21].

2), then the excitation energy distribution of residual nuclei will be wide too. In this approach, the excitation energy of the nucleus is the sum of "particle" and "hole" energies measured from the Fermi level. Then, from the energy balance, we have

$$E^* \simeq m_\pi - \sum_i (T_i - \bar{B}_N) \qquad (12)$$

where T_i is the kinetic energy of the i-th cascade nucleon in the laboratory system; $\bar{B}_N$ = 7 MeV is the mean binding energy of a nucleon in the nucleus.

In Fig. 6 the distribution of the excitation energy for residual nuclei before the evaporation stage is given as an example. For the heavy Pb nucleus, the excitation energy varies in a wide range from several MeV to 140 MeV, that corresponds to full absorption of all cascade particles and transformation of the whole pion mass into the excitation energy of the nucleus. For a light nucleus $W(E^*)$ distribution becomes narrower and its maximum shifts to lower values of E^*.

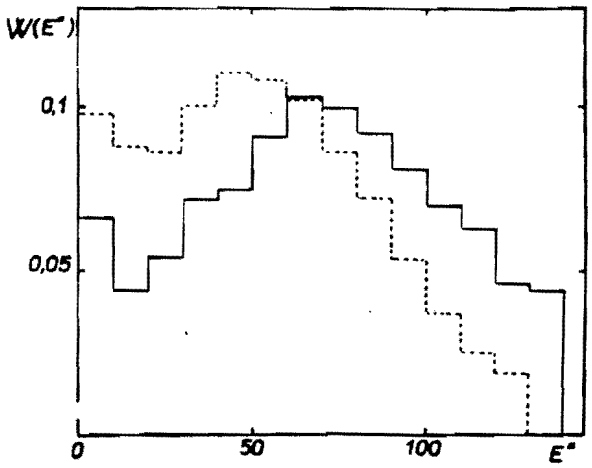

Fig. 6.
Distribution of residual nuclei formed after pion absorption by ^{31}P (dots) and ^{208}Pb (solid histogram) with respect to excitation energy E* (in MeV).

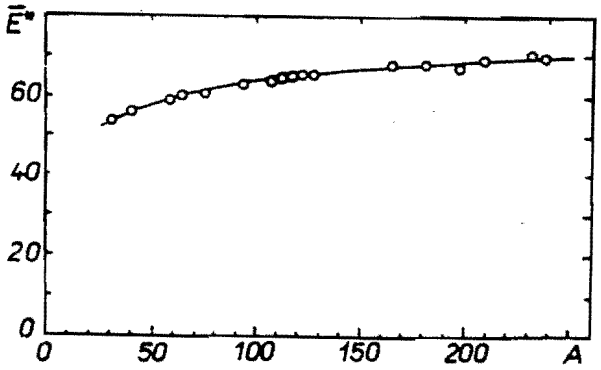

Fig. 7.
Mean excitation energy $\overline{E^*}$ (MeV) of residual nuclei in π^--capture vs. mass number A of the nucleus target. Smooth curve is drawn through calculation points by eye.

Mean excitation energy increases with increasing mass number A of the nucleus-target (see Fig. 7). Therefore, the heavier is the nucleus--target, the wider the isotope yield curve.

In Figs. (8-12) experimental yields of reactions (π^-, $xn\,yp$) are compared with the calculations performed by models /1-3/. The models are equally successive in describing the main feature of nuclear disintegration following π^--absorption. This may presumably be explained by a great contribution of the evaporation stage, which is present in all models and is equally described, to the production of the given final isotope. It is therefore natural that the differences in various models must affect most greatly the yields of reactions with emission of small number of particles. In approaches /1,3/ considering the surface nature of absorption these yields must exceed the results of the exciton model /2/. In the case of reaction (π^-, xn), the data calculated by the cascade-evaporation model prove to be lower than the experimental ones at $x > 12$ (see Figs. 10-12). As is shown in /1/ this may indicate a possible contribution of α-particle absorption mechanism.

In the case of light and medium targets, emission of charged particles contributes greatly (Table I). The Coulomb barrier of heavy nuclei hinders emission of charged particles at last stages of the process and the reaction (π^-, xn) prevails here. The (π^-, pxn) yield in the region of heavy nuclei will be less than the (π^-, xn) yield but compa-

Fig. 9.
Isotope yield following pion absorption by ^{59}Co nuclei. Experimental data are taken from [20]. Histogram, authors calculation; solid curve, calculation by the exciton model [30].

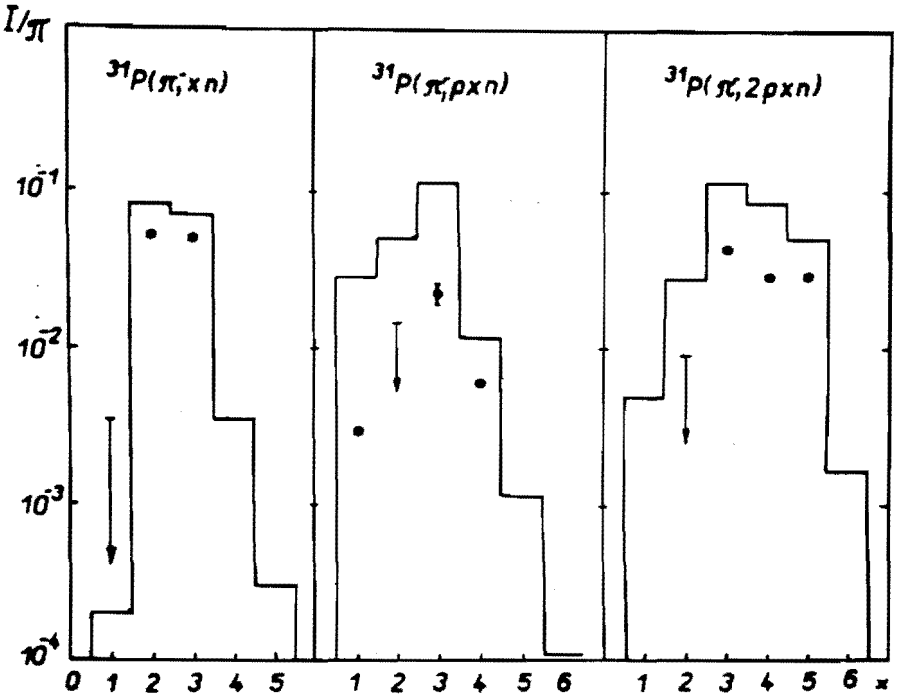

Fig. 8.
Isotope yield following pion capture in ^{31}P nuclei. Experimental data are taken from [52]. Histogram, authors calculation.

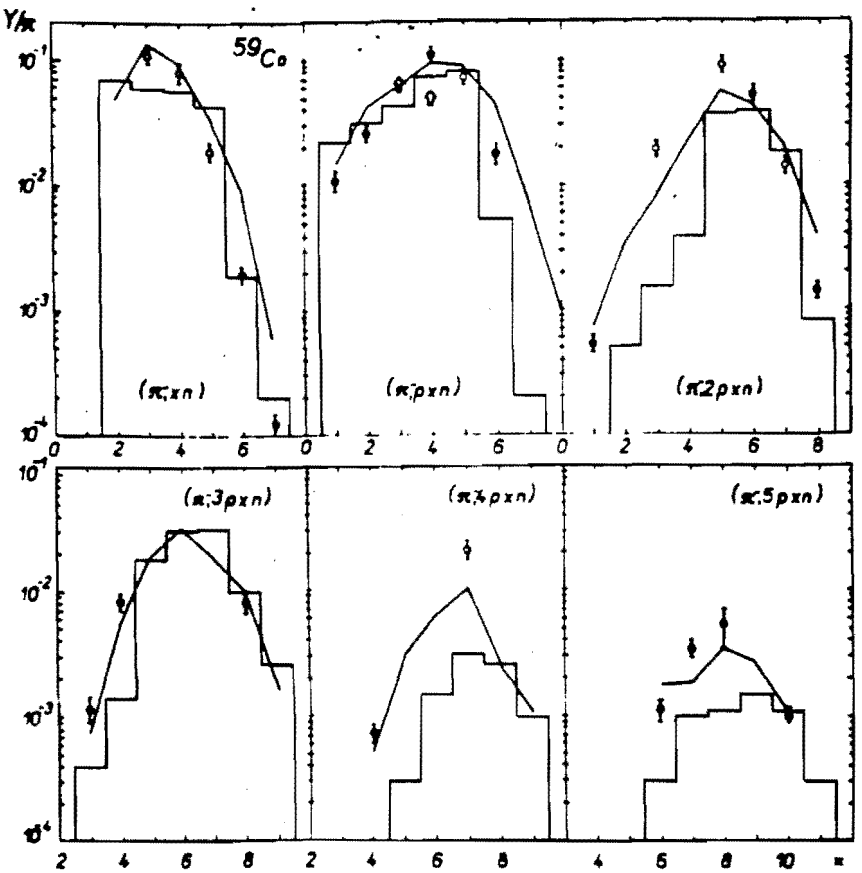

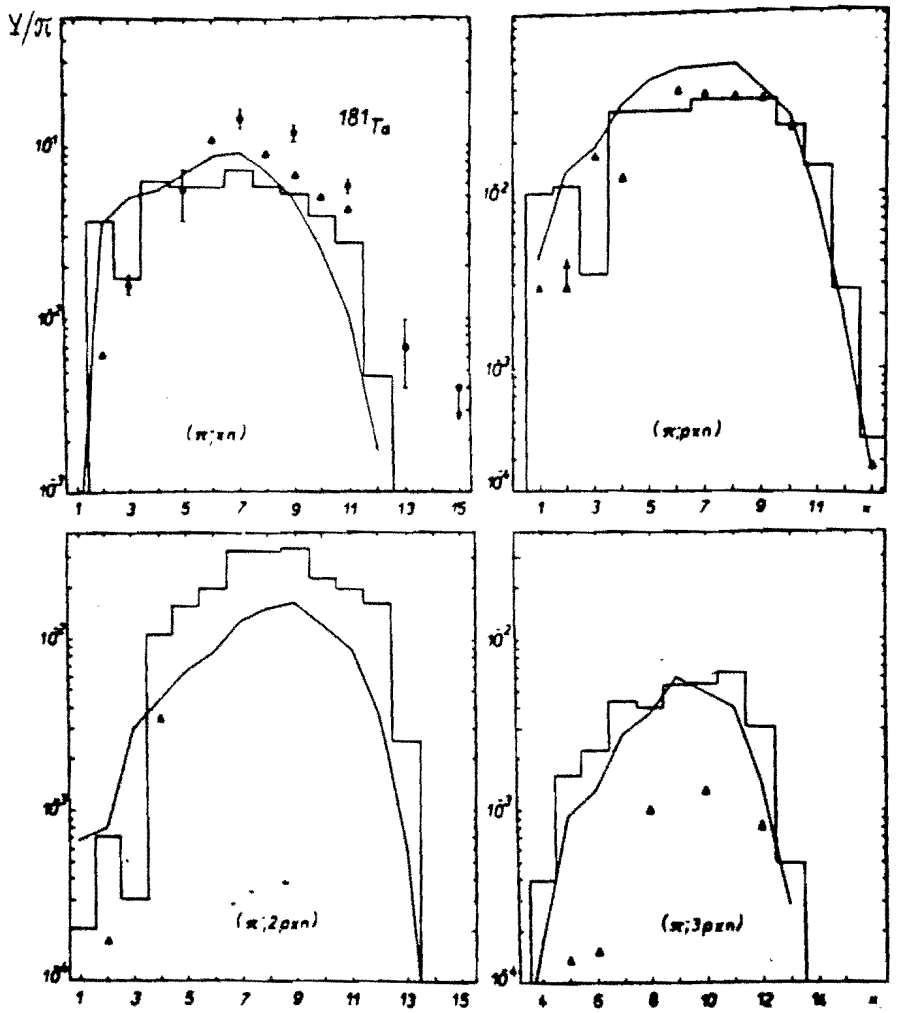

Fig. 10.
Isotope yield following pion absorption in ^{181}Ta nuclei. Experimental data are taken from [3] (triangle) and [58] (circles). Histogram, authors calculation; solid curve, calculation [3].

rable in value, since the Coulomb barrier has no effect on the emitted proton after pion absorption in the p-p pair. In general, the relationship between xn- and pxn-yields on heavy nuclei may therefore give information on the value of $R = W_{n-p} / W_{p-p}$. However, the solution of this problem requires in addition more exact experimental data and more detailed investigation of the effect of different model parameters on the (π^-, xn)- and (π^-, pxn)-yields.

3.5. Excitation of High Spin States and Angular Momenta of Residual Nuclei

It is found in /60/ that following pion absorption in heavy nucleus-target. metastable states of residual nuclei whose spin achieves

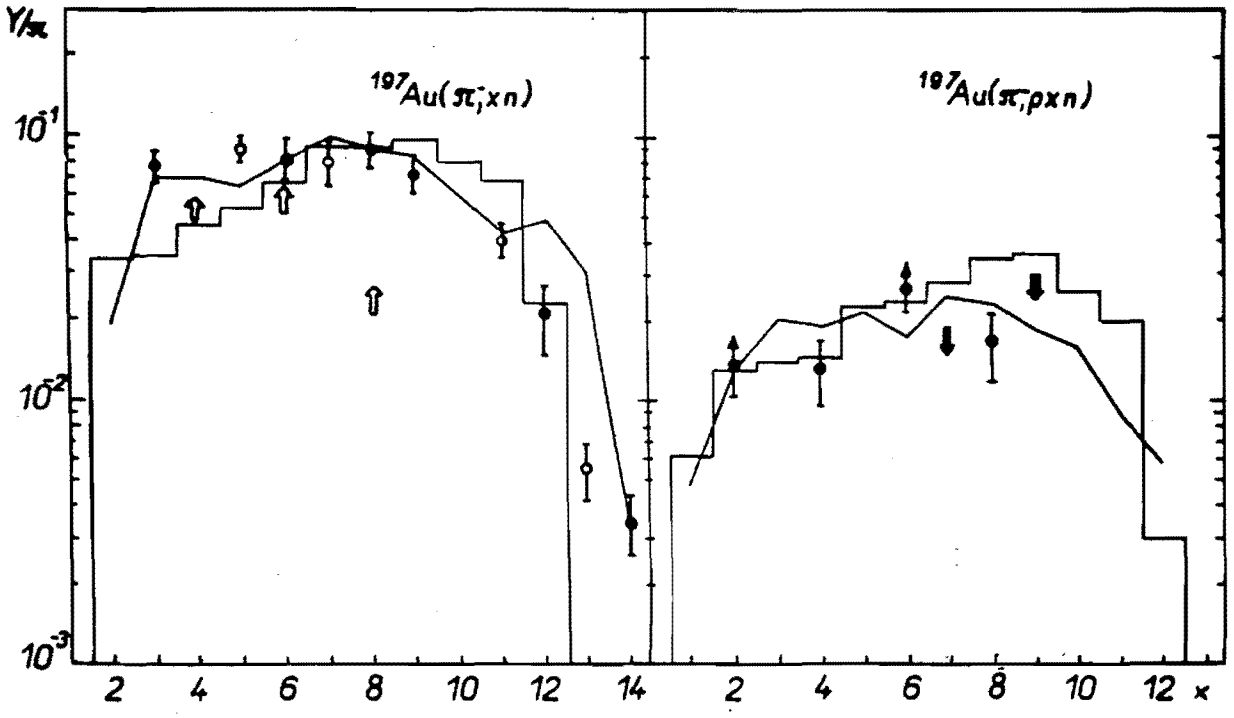

Fig. 11.
Isotope yield upon pion absorption in ^{197}Au nuclei. For notations, see Fig. 9.

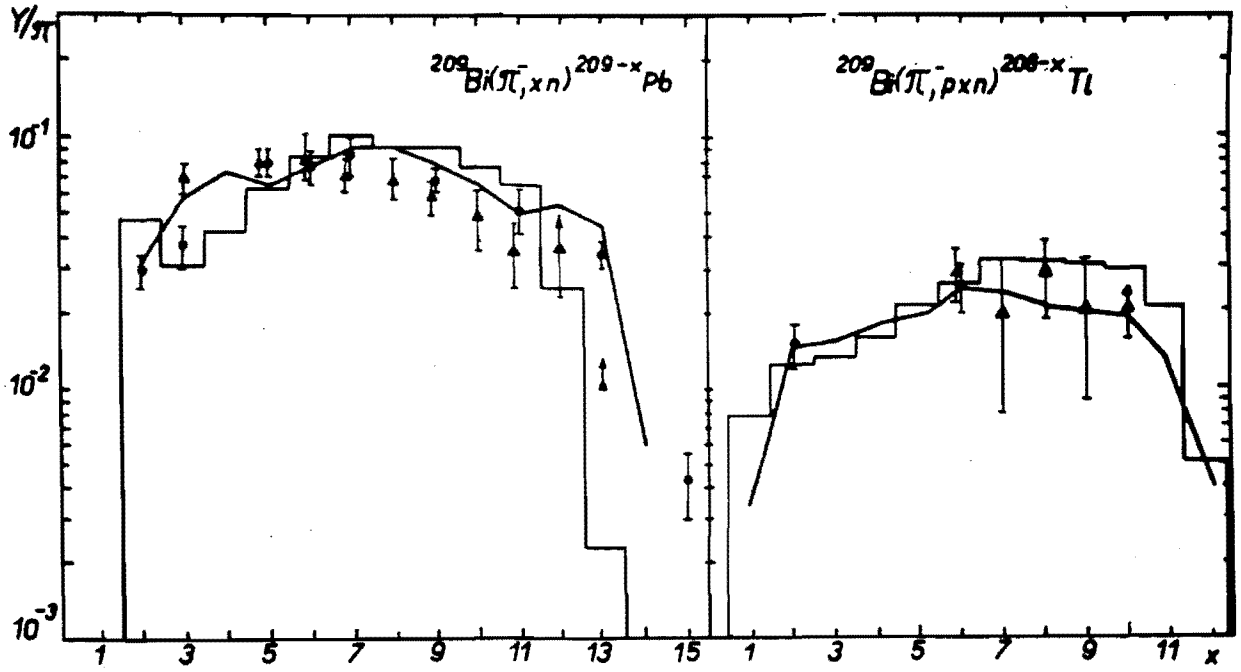

Fig. 12.
Isotope yield upon pion absorption in ^{209}Bi nuclei. Experimental points are taken from [30] (triangles) and [58] (circles). For notations, see Fig. 9.

Table 1

Experimental and theoretical yields (%) of different reaction channels in the absorption of stopped negative pions by ^{59}Co and ^{197}Au nuclei

Reaction	^{59}Co			^{197}Au		
	experiment /30/	present work	calcul. /30/	experim. /30/	present work	calcul. /30/
(π^-,xn)	24 ± 3	23.2	34.0	74 ± 8	69.0	73.6
(π^-,pxn)	32 ± 3	25.4	35.9	20 ± 7	23.6	18.9
$(\pi^-,2pxn)$	24 ± 3	30.9	16.1			
$(\pi^-,3pxn)$	12 ± 4	9.75	9.3			
$(\pi^-,4pxn)$	6 ± 2	9.34	3.4			
$(\pi^-,5pxn)$	1.5±0.2	0.86	1.2			

10-20$\hbar$ are excited intensively. These experiments excite great interest. It was unclear how such high angular momentum of residual nuclei appear, if the orbital momentum, ℓ , of the pion on the mesoatomic orbit from which absorption occurs, is small ($\ell \leq 3\hbar$). Therefore, a great number of experiments /3,30,50-52,55,56,58,61,62/ dealing with this phenomenon have been performed for a short time.

This phenomenon has been explained in /1/. Later its similar interpretation has been given in /3,64,65/. It is shown that most nucleons emitted from the surface layer of the nucleus at the stage of an intranuclear cascade are responsible for the large angular momentum of the residual nucleus. If we make the most unfavorable assumptions, i.e. neglect the orbital pion momentum and spins of the nucleus and particles, we shall obtain

$$\vec{M} = -\sum_i \vec{m}_i \qquad (13)$$

from the law of angular momentum concervation.
Here M is the angular momentum of the residual nucleus; m_i is the angular momentum carried away by a cascade particle. In Fig. 13 distribution of residual nuclei over the absolute value of the angular momentum is given. In the case of heavy nuclei-targets, residual nuclei, whose angular momentum may achieve 15-17$\hbar$, are produced following intranuclear cascade stage. So, with regard for spin and orbital momentum due to the pion, the spins of residual nuclei may exceed 20$\hbar$. High angular momenta of residual nuclei such as these are comparable with the value of M obtained in reactions with heavy ions. While in reactions with heavy ions the angular momentum is introduced by an incident

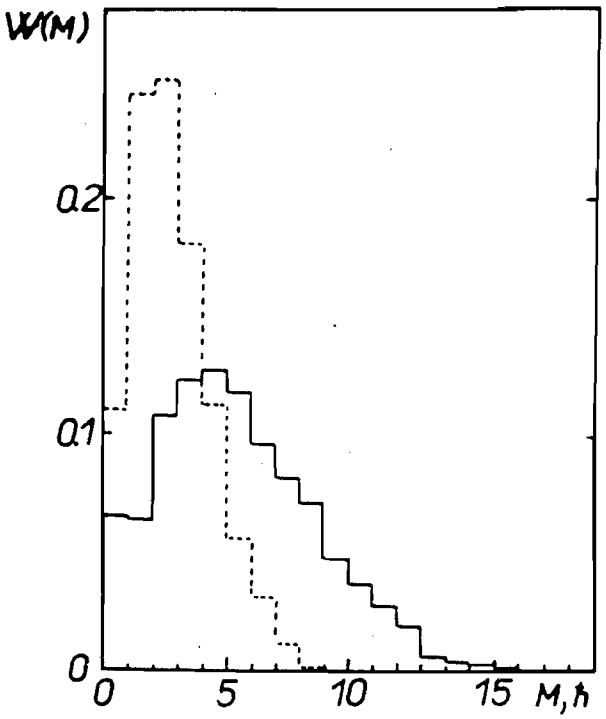

Fir. 13.
Distribution of residual nuclei formed following pion absorption in ^{31}P (dots) and ^{208}Pb (solid histogram) nuclei with respect to the angular momentum M.. Each distribution is normalized for one pion absorption.

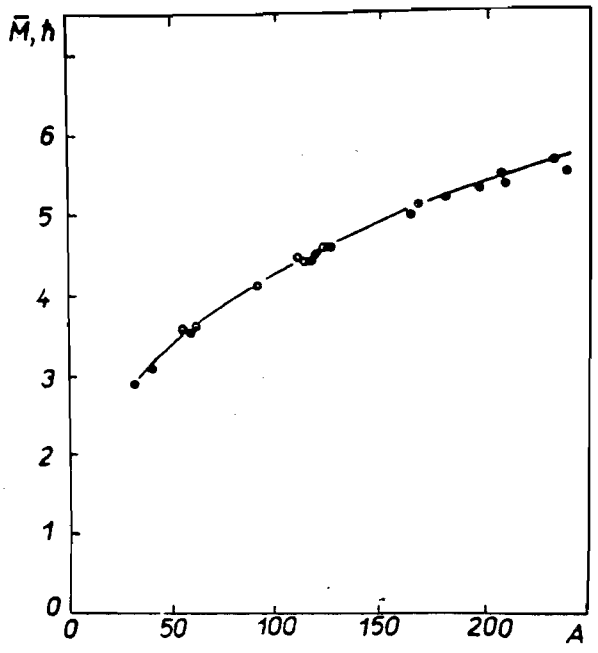

Fig. 14.
Mean angular momentum $\bar{M}$ (in $\hbar$ units) vs atomic number of the nucleus-target A. Points, calculation results; solid curve, approximation $\bar{M} = 0.92\ A^{1/3}$.

particle, then in reactions with pions the additional angular momentum is created due to emission of fast particles from the surface nuclear layer.

It is known that during particle evaporation the initial angular momentum of the compound nucleus changes insignificantly. Therefore, to the first approximation the distribution given in Fig. 13 may be related to the nuclei produced after the evaporation stage. Then it becomes clear why in reactions of pion absorption in heavy nuclei isomers with spin $\sim 18\hbar$ are populated. The heavier the nucleus, the higher spin states of the residual nucleus may be populated, since distribution over M in the case of light nuclei shifts to the region of small M. In Fig. 14 mean angular momentum of residual nuclei and the atomic number of the nucleus-target are related by the law $M \simeq 0.92A^{1/3}$, which is a direct reflection of the surface nature of stopped pion absorption in the nucleus.

The excitation of the high-spin state may be observed not only in pion absorption by nuclei, but also in other processes involving emis-

sion of fast particles from the nucleus. First of all, it is K^--meson and antiproton absorption from the orbits of hadronic atoms which mainly proceeds in the surface layer. High-spin states of residual nuclei must be excited as well in reactions of nuclear spallation by intermediate energy particles.

It should be noted, however, that total distribution of residual nuclei with respect to the angular momentum cannot be considered as rather a sensitive characteristic whose study may give information on the mechanism of absorption of various particles in nuclei. This statement was supported in /66/ by comparing two similar reactions, i.e. absorption of stopped pions and γ-quanta with energy $E_\gamma = m_\pi$. The mechanism of γ-quanta absorption at such energy is well known to be quasideuteronic, but unlike pions, γ-quanta absorption proceeds uniformly over the whole nuclear volume. Calculations /66/ have shown that in both reactions angular-momentum distributions of residual nuclei are similar (see Fig. 15). Theoretical study /3/ of proton-nucleus interaction with $E = m_\pi/2$, which is similar to pionic absorption, has also indicated similarity in nucleus distribution with respect to the value of M .

Experiments /7/ have shown that the value of isomeric ratio depends both on the spins of ground and isomeric states, and on the number of emitted particles. It is therefore difficult to determine the shape of the angular momentum distribution of residual nuclei from fragmentary measurements. In /1,66/ it is suggested to use the dependence of the average angular momentum M (or consequently, the isomeric ratio R_i for rather large fixed nuclear spin) on the number, x, of particles emitted in order to study the absorption mechanism. It can be easily shown that not all the x values are equally effective for the popula-

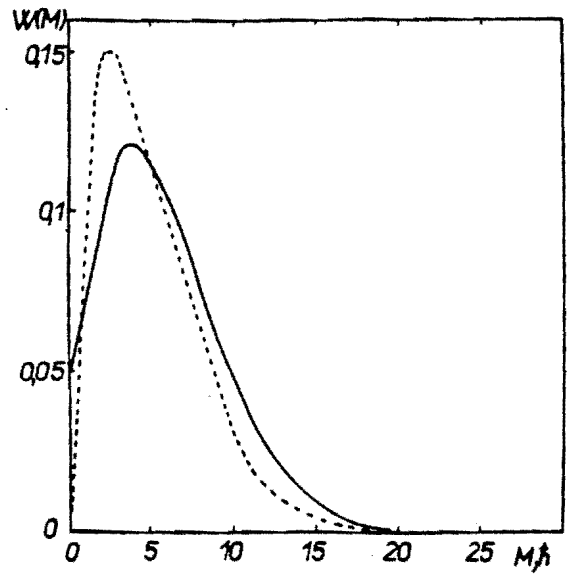

Fig. 15.
Distribution of residual nuclei formed following absorption of slow pions (solid curve) and γ-quanta with E_γ = 140 MeV (dots) with respect to the angular momentum M.

tion of high-spin states. As an example, consider reaction (π , xn). The case of maximum x when all of the cascade particles are absorbed in a nucleus and then only neutrons are evaporated from it isotropically, corresponds to low values of M (see formula (13)). Another extreme case x=2, when after absorption in n-p pair two neutrons fly apart in opposite directions, also yields a low value for the angular momentum of the residual nucleus. The maximum angular momentum will be presumably realized when, following absorption in the surface layer, one fast nucleon goes away without collisions, while the second is absorbed in the nucleus. In this instant, the compound nucleus with the excitatinn energy $E^* = m_\pi/2$ will emit, on the average, 5-6 evaporation neutrons. Thus, in the case of surface absorption the dependence of the mean angular momentum M(x) will have its maximum at x 6-7 (see Fig. 16). For the volume absorption of γ-quanta, the dependence $\bar{M}(x)$ will have another form at low x (see Fig. 16).

Experiments have shown that the probability of excitation of high-spin isomers depends really on the number of emitted neutrons approximately in the same way as theory predicts. In /62/ the study is made of the dependence of the probability of producing high-spin indium isomers $^{108m}In(7^+)$ and $^{110m}In(7^+)$ on the number of neutrons emitted at π^--absorption by ^{112}Sn, ^{114}Sn, ^{116}Sn, ^{118}Sn, ^{120}Sn, ^{122}Sn and ^{124}Sn nuclei. The values of isomeric ratio σ_m/σ_g in arbitrary units vs the number of neutrons emitted are given in Fig. 17. The isomeric ratio is

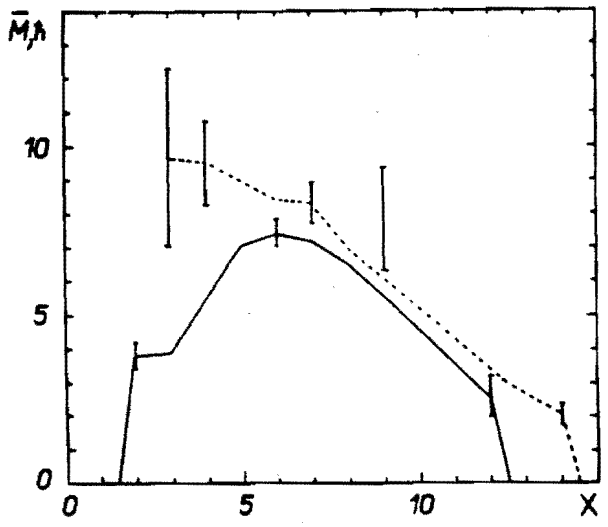

Fig. 16.
Mean angular momentum $\bar{M}$ vs the number of particles emitted in reaction (π^-, xn). Solid curve, calculation [66] for ^{208}Pb (π^-, xn) reaction; dots, for ^{208}Pb (γ, xn) reaction. Statistical errors of the calculation are shown in this figure.

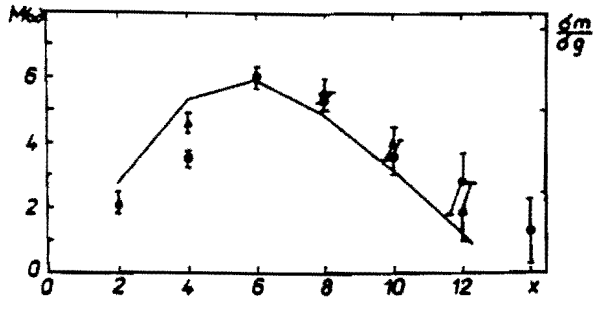

Fig. 17.
Isomeric ratio σ_m/σ_g and mean angular momentum $\bar{M}$ vs the number of emitted particles in reaction $Sn(\pi^-, xn)$. Experimental points are taken from [62]: circles, ^{108m}In (7^+); triangles, ^{110m}In (7^+). Curve, calculation results.

seen to increase with increasing multiplicity, and then to fall with further increase of x. The data obtained give clear manifestation of the surface nature of stopped pion absorption in two-nucleon associations.

The studies /1,3,63-65/ seem to indicate that fast nucleons emitted at the stage of intranuclear cascade present the main source of high angular momentum for the residual nucleus in pionic absorption. However, it would be rather captivating to investigate other mechanisms of high angular momentum of residual nuclei. In particular, the nucleus may acquire high value of M after emission of a complex charged particle with the energy above 50 MeV. As seen from Fig. 3, however, the probability of this process will be less than 10^{-4}. Fluctuation is another possible mechanism, when a large angular momentum of the residual nucleus may be produced due to random addition of momenta carried away by with evaporated particles. Perhaps, some hints as to such a mechanism may be found in /58/ where it is observed that emission of 13 neutrons following pion absorption in ^{181}Ta nucleus excite the states with the spin 16 $\hbar$ (with the probability $\sim 10^{-3}$ per 1 pion).

Thus, the method of studying the mechanism of stopped pion absorption in nuclei through excitation of high-spin nuclear states is far from exhausting all its possibilities. As to other nuclear reactions initiated with intermediate energy particles, no systematic studies of the angular momenta for residual nuclei are available.

3.6. Momentum of Residual Nucleus

It is seen from the above that the study of nucleus angular momentum presented valuable information on the mechanism of pion absorption in the nucleus. Momentum $\vec{P}$ is its another important characteristics. Within the light nuclei region the absorption products are emitted mainly without interaction with intranuclear nucleons, therefore measurements of the nucleus momentum make it possible to determine the momentum of multinucleon association absorbing a pion. Great contribution of secondary processes accompanying pion absorption in complex nuclei makes the situation more intricate. The momentum of the nucleus-target will depend on different reaction characteristics as, for example, on the number of nucleons emitted ΔA.

For the simplest reaction (π^-, $2n$) the nucleus momentum may be extracted from the analysis of the kinematically complete experiment involving measurement of the energies of two neutrons /41-43/. Measurement of nuclear momentum in terms of the Doppler effect may be used in general for a wider set of residual nuclei /52,59,67-69/.

In models /1,3/ the nucleus momentum is determined by the simple relationship

$$\vec{P} = -\sum_i \vec{p}_i \qquad (14)$$

where p_i is the momentum of a secondary particle. The calculations in the frameworks of model /1/ have shown that the mean momentum of the residual nucleus does not practically depend on the mass number of the nucleus-target and is equal to $\bar{P} \approx 220$ MeV/c. In contrast to the angular momentum, distribution of the momentum of residual nuclei slightly depend on the nucleus-target (see Fig. 18).

In Fig. 19 the calculated dependence of the mean nucleus momentum $\bar{P}$ vs the number, ΔA, of nucleons removed from the target following pion absorption in it, is compared with experiment. For small values of $\Delta A \leq 4$, the momentum increases with increasing ΔA and then is slightly dependent on ΔA. The results of calculation in the case of no

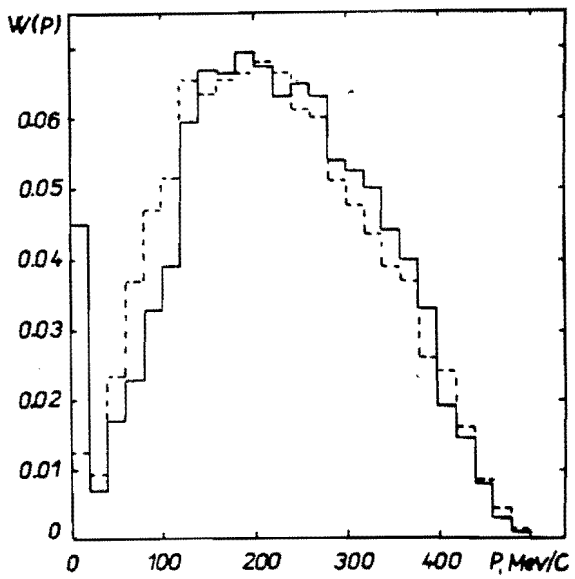

Fig. 18.
Momentum distribution for residual nuclei formed after π^--absorption in ^{31}P (dots) and ^{208}Pb (solid histogram) nuclei.

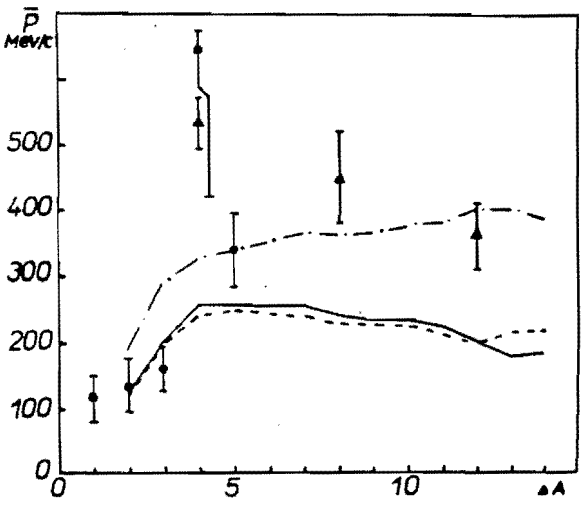

Fig. 19.
Mean momentum $\bar{P}$ of the residual nucleus vs the number of nucleons emitted from the nucleus-target. Experimental data for ^{31}P nucleus-target (circles) and ^{40}Ca target (triangles) are taken from [52, 59]. Solid curve, calculation for ^{40}Ca, dots, for ^{31}P. Dotted-dashed curve, calculation for ^{40}Ca with allowance for pre-equilibrium particle emission and evaporation.

pre-equilibrium emission and evaporation lie below the experimental $\bar{P}$ values at high ΔA. The consideration of the momenta of pre-equilibrium and evaporated particles improves the agreement with the experiment (see Fig. 19), some of the points, however, remaining above the theoretical curve. But one cannot neglect that the possibility of the experimental data to be overestimated since it is necessary to prescribe the shape of the momentum distribution of the nucleus target when extracting $\bar{P}$. For easier estimation of $\bar{P}$ by formula (14), it is worth noting that the momentum of the nucleon with $E_n = m_\pi$ is 510 MeV/c, while for $E_n = m_\pi/2$, the nucleon momentum is 360 MeV/c.

The experiments started in /52,59,67-69/ require further elaboration concerning both methods and measurements of other nuclear reaction characteristics. For example, when measuring the mean nucleus momentum for the states with different fixed values of the spin M based on the Doppler effect, the dependence of $\bar{P}$ on the angular momentum of the nucleus may be determined.

3.7. Nuclear Fission Following Absorption of Stopped Pions

Highly excited compound nuclei can de-excite not only through particle emission but by fission as well. When stopped π^--mesons are absorbed, not only highly fissionable nuclei with mass $A > 230$, but also slightly fissionable nuclei with $A < 200$ can undergo fission since the excitation energy can reach a value of 140 MeV. Really, in experiments /70-75/ both heavy and medium-weight nuclei undergo fission by stopped pions.

For highly fissionable ^{235}U, ^{238}U and ^{232}Th nuclei, whose fissility is about several tens percent, the competition between particle evaporation and fission affects various reaction characteristics. One of these is isotope yield. As shown in /1/, fission must cause drastic contraction of the isotope yield curve. Since nuclear fissility increases markedly with decreasing number of neutrons /17/, the fraction of neutron-deficient nuclei escaping fission decreases sharply (see Fig. 20). Therefore the broadening of the isotope yield curves for the targets with $62 \leq A \leq 209$ observed in /30/ must cease with further growth of the mass number replaced by their narrowing in Th and U region. Unfortunately, the isotope yield curve for highly fissionable targets has not been measured yet. The only experimental point /54/ on the curve of the isotope yield from the thorium target agrees with the calculations and supports the general trend to decreasing yield of neutron-deficient isotopes. Thus, fission greatly restricts production of neutron-deficient isotopes on uranium and transuranium targets.

Fig. 20.
Actinium isotope yield per one absorbed pion in reaction $^{232}Th(\pi^-, xn)^{232-x}Ac$. Solid and dotted histograms, calculation with neglect of and with regard for fission ($a_f/a = 1.07$). Experimental point is taken from [54].

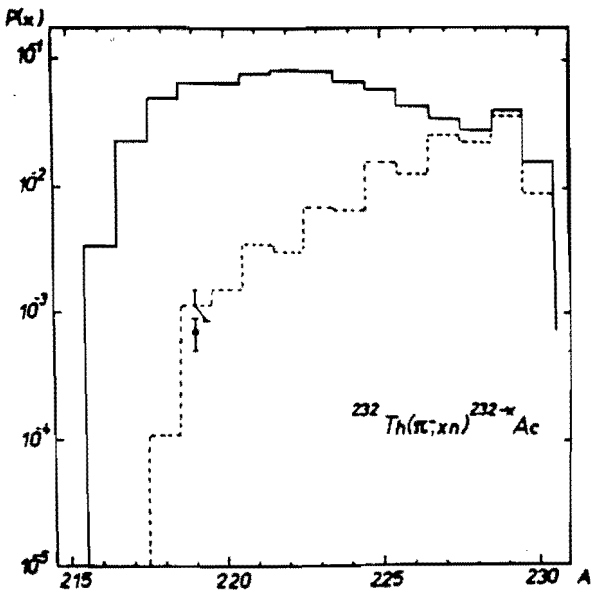

Nuclear fissility with slow pions decreases with decreasing atomic number A of the nucleus target (see Fig. 21). The A-dependence of the fissibility has been analysed in /1,22,76/. It is shown that experimental fissilities of nuclei by pions may be described within the framework of the quasideuteron absorption mechanism using either methods of calculation of nuclear fission by intermediate energy protons /1/ or the fission barriers B_f taken from the experiments with low-energy particles /22,76/. It is shown in /22,76/ that calculated fissilities of nuclei by pions are rather sensitive to the ratio of the level density parameter for the saddle point and excited state a_f/a. In order to describe the experimental data, the authors of /22/ applied $a_f/a = 1.2$, while in /76/, $a_f/a = 1.1$ was obtained. It should be noted that similar values of a_f/a are obtained in experiments of fission of highly excited compound nuclei formed in reactions with low-energy α-particles /77,78/. These conclusions are in agreement with the results of theoretical analysis of nuclear fissility with intermediate energy protons /79/, where high sensitivity of fissility to the value of a_f/a is also emphasized. The value $a_f/a = 1.05$ founded in /79/ for 150 MeV protons agrees with the results of /76/. The value of $a_f/a = 1.2$ from /22/ seems to be overestimated possibly due to very simplified model used for description of the pion absorption in the nucleus.

For the time being, however, when pion absorption in nuclei is well-studied, another statement of the problem becomes more topical: what kind of new information may be obtained by analysing the results of nuclear fissility measurements? This is closely connected with the answer to the question what other details of the process may affect the value of the fissility.

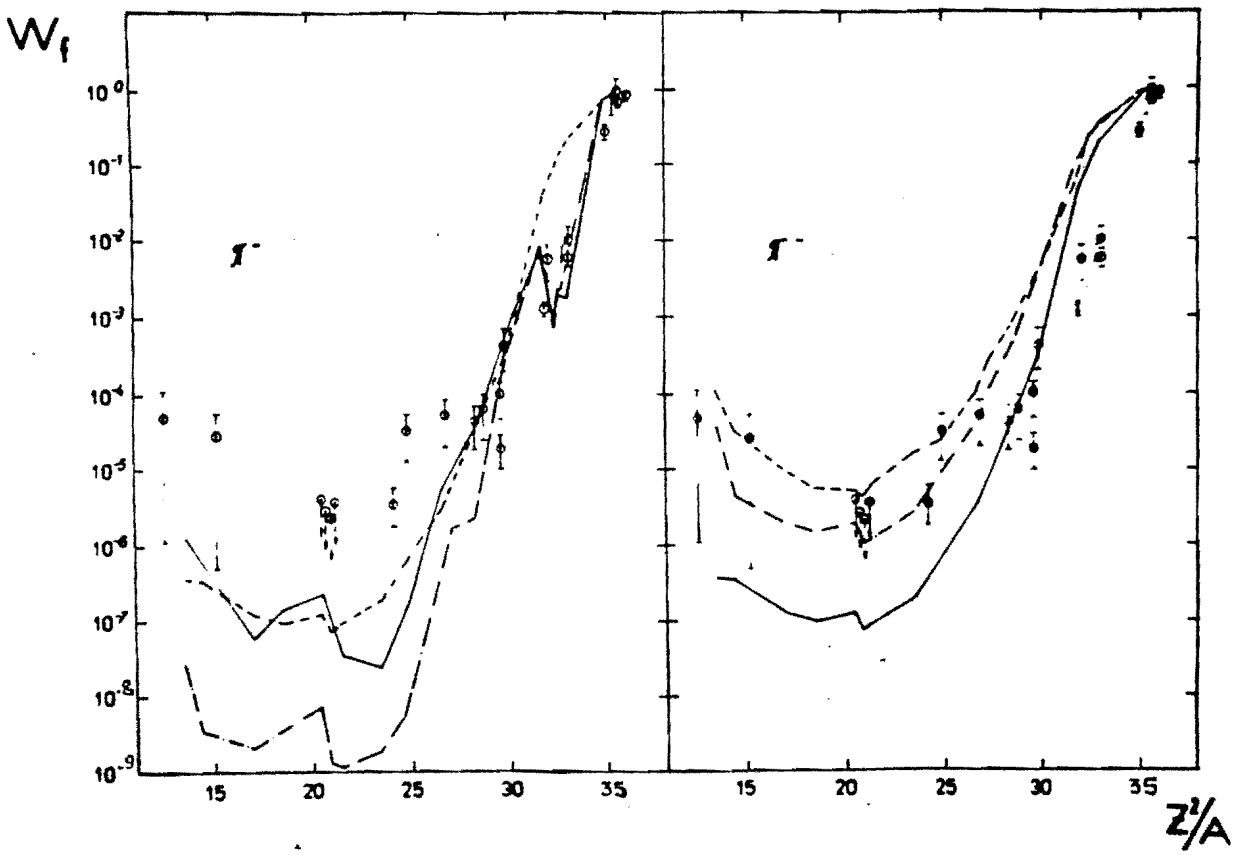

Fig. 21.
Nucleus fissility W_f as a function of Z^2/A for the nucleus-target. Experimental points, data of [74] (circles) and [75] (triangles). Left-hand side; Solid curve, calculation with the barriers of Swiatecki et al [80, 81] for $a_f/a = 1.1$. Dots, calculation for the same parameters with neglect of the shell effects. Dotted-dashed curve, calculation for $a_f/a = 1.2$ and with allowance for pre-equilibrium particle emission. Right-hand side; solid curve, calculation with the barriers of Swiatecki et al. [80, 81] for $a_f/a = 1.1$ with neglect of shell effects. Dots, calculation with the same set of parameters but with the barriers of Krappe and Nix [83]. Dotted-dashed curve, calculation with allowance for "thermal" effects.

In the first place, the analysis of nuclear fissility by pions may give information on the value of fission barriers in the unstudied region of medium and light nuclei. Up-to-date fission models predict that with a decreasing mass number A the height of the fission barriers must increase achieving its peak B_f^{max} at $A \simeq 80$–100 and then decrease in the region of light nuclei (see Fig. 22). In view of this, in /84/ it has been predicted that nuclear fissility must diminish to some minimum value at $A \simeq 80$–100 and then grow again in the region of light nuclei. To discover this growth of fissilities, a great number of experiments have been performed on nuclear fission by intermediate energy γ -quanta, protons and α -particles. These works, however, involve great difficulties due to great contribution of background processes like fragmentation of nuclei-targets. At the same time, the studies with stopped negative pions have great advantages since in these case

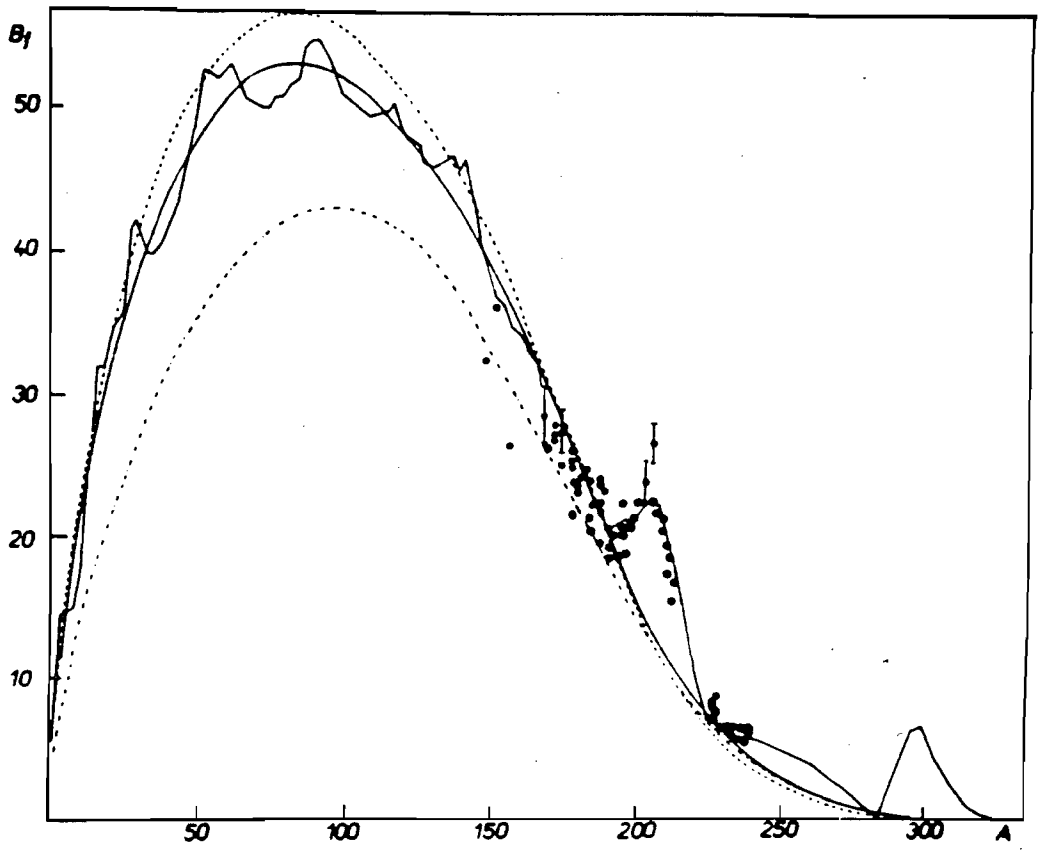

Fig. 22.
Nuclear fission barrier heights (MeV) along the beta-stability line. Solid curves, calculation by the liquid drop model of Swiatecki et al [80,81] with regard for and with neglect of the shell correction. Dotted and dotted-dashed curves, calculation by the liquid drop model with the parameters of Pauli and Ledergerber [82] and by the modified liquid drop model of Krappe and Nix [83] with neglect of shell corrections.

the transfer of high excitation energy to the nucleus involves minimum contribution of such processes as fragmentation *.

In Fig. 21, the results are presented of the analysis of nuclear fissility with pions obtained in the framework of model /1/. To describe the fissility for heavy and medium-weight nuclei ($Z^2/A \geq 27$) based on the widely-used liquid drop model of Myers, Swiatecki /80/, the ratio $a_c/a = 1.1$ must be taken as in /76/. In the region of the double-magic ^{208}Pb nucleus appreciable discrepancy with the experiment indicates the necessity of more rigorous allowance for the shell effects in the densi-

* It is of interest to extend the pioneer experiments on nuclear fragmentation with pions /85/ to the region of low energies where no data are available.

ty of nuclear levels. A convenient approximation for the level density parameter is obtained in [86]

$$a(E^*,A,Z) \simeq \tilde{a}\left[1+(1-e^{-0,061\,E^*})\,\Delta M/E^*\right] \qquad (15)$$

where ΔM is a shell correction for the nuclear mass; $\tilde{a} = 0.134 - 1.21\cdot10^{-4}\cdot A$ is an asymptotic value of the level density parameter.

As has been shown in [1,79], the medium-weight nuclei fissility is greatly affected by the pre-equilibrium emission of particles from the residual nucleus. Those nuclei undergo fission at first stages of the evaporation cascade when the compound nucleus still possesses high excitation energy. Emission of a pre-equilibrium particle appreciably lowers the excitation energy of the compound nucleus and, hence, decreases the probability of its fission. It follows from Fig. 21 that uncertainties in describing thermalization of the residual nucleus may cause as much as 10-fold change in the fissility of medium and light-weight nuclei. In the region of medium-weight nuclei the higher value of $a_f/a = 1.2$ must be taken in order to compensate the fissility decrease.

However in the region of nuclei with $Z^2/A \leq 27$ the calculated fissilities lie below experimental values. The above uncertainties of the model may only increase this discrepancy. The latter may be due to the fact that the parameters of the liquid drop model are fixed insufficiently reliably which leads to high values of B_f when extrapolating to the unknown region of light and medium weight nuclei. In the model of [80,81] the maximum fission barrier $B_f^{max} = 52$ MeV, while in the model of [82], $B_f^{max} = 56$ MeV (see Fig. 22). For better description of experimental fissilities, modified liquid drop model of [83] with $B_f^{max} = 43$ MeV* must be preferred. Such a decrease in fission barriers leads to about 50-fold increase in the pionic fissility for light and medium weight nuclei (see Fig. 21).

Another physical effect that may probably eliminate the discrepancy is reduction of the fission barrier height with increasing energy of excitation. The calculations by the methods of Tomas-Fermi [88] and Hartree-Fock [89] predict that "thermal" effects must lead to B_f decrease. This is most appreciable for medium weight and light nuclei with the energies of excitation above 50 MeV (see Fig. 23). "Thermal" effects may cause about 10-fold increase in nuclear fissility with $Z^2/A \leq 27$ (see Fig. 21).

The measurement of nuclear fission with slow negative pions makes it possible to verify an another prediction of the liquid drop model,

* The description of experimental fissilities for light and medium weight nuclei is the most difficult in the case of droplet-model giving the maximum fission barrier height $B_f^{max} = 80$ MeV [87].

Fig. 23.
Variation of the nuclear fission barrier (MeV) in the liquid drop model along the beta-stability line with increasing excitation energy.

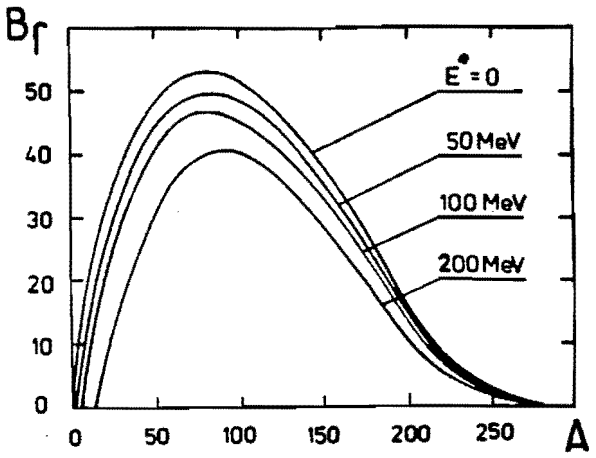

namely, the existence of a critical point where fission of light nuclei is replaced by the process similar to fragmentation. The liquid drop model /80,81/ specifies the position of the critical point at $(Z^2/A)_{cr}$= 19.8, while the modified liquid drop model /83/, at $(Z^2/A)_{cr}$=23.8 and droplet model /87/, at $(Z^2/A)_{cr}$=32.0. The verification of this prediction requires more reliable experimental methods to measure the kinetic energies of fission fragments in coincidence.

4. Contributions of Various Mechanisms of Pion Absorption in the Nucleus

The comparison between the experiment and calculations based on the quasi-deuteron absorption mechanism shows the predominance of this mechanism. However, a number of characteristics exhibit discrepancy between theory and experiment that can be considered as indication of some possible contribution of other absorption mechanisms.

Single nucleon absorption may manifest itself in the energy spectrum of nucleons, since in this case a nucleon must posses maximum energy as compared to nucleons formed in other mechanisms. In the case of light nuclei, single nucleon absorption gives rise to a peak in the high-energy "tail" of the spectrum. The probability of single nucleon absorption measured in this way /90/ is $\sim 10^{-3}$. In the region of heavy nuclei, due to high density of excited states of residual nuclei, it is impossible to identify the peak corresponding to single nucleon absorption. The probability for single nucleon absorption may be estimated only indirectly as a deviation of experimental data from the calculations based on the two nucleon absorption mechanism. As is seen from Fig. 2, rough estimation gives for the value of the single nucleon absorption probability $\leq 10^{-3}$.

More accurate estimates for the probability of single nucleon absorption in heavy nuclei may be obtained by the activation methods. The yields of reactions (π^-, n) and (π^-, p) measured in /91,92/ also prove to be small and equal to $\sim 10^{-3} - 10^{-4}$*.

α - particle absorption. In general, pion can be absorbed not only by a two nucleon but also by any other multi-nucleon associations, for example, by ^{3}He, ^{4}He, ^{4}Li, etc. At present, for the region of light nuclei, the α -particle absorption mechanism suggested in /93/ is most comprehensively studied. The analysis of experimental data /94/ implies that in light nuclei the probability for α -particle absorption can amount to $\sim$ 20-30%. For the region of medium weight and heavy nuclei the role of the α -particle mechanism is not studied yet.

For the time being, only one estimation /1/ of the contribution of the α -particle mechanism of pion absorption by complex nuclei has been performed. In this case the following channels for reaction with relative probability ω are possible /95-96/

$$\pi^- + {}^4\mathrm{He} \rightarrow t + n \qquad \omega_2 = (19 \pm 1)\% \qquad (16a)$$

$$\pi^- + {}^4\mathrm{He} \rightarrow d + 2n \qquad \omega_3 = (58 \pm 7)\% \qquad (16b)$$

$$\pi^- + {}^4\mathrm{He} \rightarrow p + 3n \qquad \omega_4 = (26 \pm 6)\% \qquad (16c)$$

In /1/ a simplification is used according to which only the channel (16c) is realized. In terms of kinematics, reaction (16c) is an extreme one with respect to reaction (4) (the pion mass is converted to the kinetic energy of four rather than two nucleons). It is natural that nucleons formed in reaction (16c) will have lower energies than in reaction (4) and will be absorbed in the nucleus with higher probability.

As a result, the α -particle absorption converts the pion mass m_π into the excitation energy, E^*, of a compound nucleus more effectively than the quasi-deuteron one /1/. Therefore the contribution of the α -particle mechanism is most distinct on the curve of the isotope yield in the region of maximum possible number of emitted particles x corresponding to the conversion of the pion mass into E^*. It should be noted that it is the case when the results of calculation in terms of the quasi-deuteron mechanism lie below the experimental data (see Figs. 10-12). Besides, for heavy nuclei, the maximum of the distributions over the number of particles emitted in reaction (π^-, xn) are distinctly divided as follows. For the α-particle mechanism it is located at x=12, and for quasideuteron mechanism, at x=7 /1/.

* Detailed discussion of the nature of single nucleon absorption is beyond the scope of the present work.

Thus, in order to determine the contribution of the α-particle absorption mechanism, it is important to study in more detail the isotope yield at large number of emitted neutrons for heavy nuclei with $A \simeq 200$.

The spectra of charged complex particles (d,t) are another source of information about α-particle absorption as the channels (16a) and (16b) contribute to the spectra. It is, therefore, necessary to generalize the simplified analysis of the α-particle mechanism in /1/ by introducing the channels with 2 and 3 particles in a final state.

As the calculations /1/ have shown, excitation of high-spin states must also be observed in α-particle absorption of pion. In this respect, channel (16a) is of interest. For this case, in the c.m.s. tritium energy will be E_t = 35 MeV, while neutron energy E_n = 105 MeV. Hence, the escape of the neutron of such a high energy from the surface nuclear layer and absorption of relatively slow tritium by the nucleus-target must involve as much as 1.25-fold higher values of angular momenta of residual nuclei than for quasi-deuteron absorption. Here, the dependence of the mean angular momentum on the number of particles emitted will have maximum at $x \simeq 4$ but not at x=7 as is the case of quasi-deuteron absorption.

Thus, even the example of α-particle absorption shows that estimation of the contribution of various multi-nucleon absorption mechanisms requires both new more complicated experiments and improvement of the theoretical models available.

5. Conclusion

The investigation of stopped pion absorption in complex nuclei not only contributes to similar investigations with light nuclei, but also allows to obtain a new unique information. For example, discovery of the phenomenon of the excitation of high-spin states in residual nuclei /60/ yielded new evidence for the surface nature of pion absorption in nuclei. The use of stopped pion absorption in the study of fission of medium weight nuclei ensures large advantages. As compared to nuclear fission by intermediate energy particles, in the case of stopped pions the contribution of background processes must be minimum. It should be noted that for the moment no measurements of fragmentation of nuclei with stopped pions are known. The further experiments would enable to choose between the fragmentation models with large input momentum as a dominating factor and those with high excitation energy of residual nuclei as a dominating factor.

For the time being two approaches are known to describe stopped pion absorption in nuclei. One is based on the exciton model /2/, the

other, on the model of intranuclear cascades [1,3]. The assumption of the quasi-deuteron pion absorption mechanism allows both approaches to describe successfully the primary reaction characteristics such as energy spectra of secondary particles, isotope yield and fission probability. However the possibilities of the second approach are greater. The allowance for the surface nature of absorption makes it possible, in addition, to describe the angular correlations of secondary particles, angular momentum and momentum of residual nuclei. Some of the characteristics require more correct calculation of the thermalization of a residual nucleus. Thus, the pre-equilibrium emission has the greatest effect on the energy spectra of charged complex particles and fission probability of the residual nucleus.

In the frameworks of the cascade approach [1], explanation was given to the phenomenon of excitation of high-spin states following pion absorption. Since high angular momenta of residual nuclei are connected with the emission of fast nucleons from the surface nuclear layer, excitation of high-spin states may be expected as well during absorption of slow K^--mesons and antiprotons. Also residual nuclei obtain high angular momenta at spallation of the nucleus-target by high-energy particles. The experiments on excitation of high-spin states can give valuable information on the mechanism of such nuclear reactions.

The analysis of experimental data performed in this work shows that in pion absorption two-nucleon mechanism is the main one. The probability for single nucleon absorption does not exceed 10^{-3} - 10^{-4} either in the region of light or heavy nuclei. The problem of the contribution of more complicated absorption mechanisms, for example, α-particle one, is still open. The presence of these mechanisms may be indicated by the discrepancy observed between theory and experiment for the yields of highly neutron-deficient isotopes and spectra of charged complex particles. In this respect, it would be of interest to detect the excitation of high spin of a residual nucleus with small number of emitted particles. The estimation of pion absorption by various multi-nucleon associations requires both new experimental information and development of the existing models.

The authors are thankful to V.M.Lobashev and V.S.Butsev for numerous discussions and valuable comments.

References

1. A.S.Iljinov, V.I.Nazaruk and S.E.Chigrinov, Preprint of INR 11-0022, M., 1975; Proc. 26 All-Union Conf. Nuclear Spectroscopy & Nuclear Structure, Nauka, L., 1976, p. 260.
   A.S.Iljinov, V.I.Nazaruk, S.E.Chigrinov, Nucl.Phys., A268, 513 (1976).

2. E.Gadioli, E.Gadioli Erba, Nucl.Phys., A256, 414 (1976);
   E.Gadioli, E.Gadioli Erba, G.Tagliaferri, Proc. Int. Conf. Nuclear Reactions Mechanisms, Varenna, Italia, June 13-17, 1977, p. 24.

3. C.J.Orth, W.R.Daniels, B.J.Dropesky, R.A.Williams, G.C.Giesler, J.N.Ginocchio, Preprint LA-UR-78-2686, Los Alamos, 1978.

4. Y.N.Kim, Mesic Atomc and Nuclear Structure, North-Holland Pub. company, Amsterdam-London, 1971.

5. D.A.Arseniev, G.G.Bunatyan, JINR P4-8835, Dubna, 1975.

6. K.H.Bruckner, R.Serber, K.M.Watson, Phys.Rev., 84, 258 (1951).

7. V.S.Butsev, Izv. AN SSSR, ser. fiz., 43, 131 (1979).

8. V.S.Barashenkov, A.S.Iljinov, N.M.Sobolevsky, V.D.Toneev. Usp. Fiz. Nauk, 16, 31 (1973).

9. M.Blann, Ann.Rev.Nucl.Sci., 25, 123 (1975).

10. E.Gadioli, E.Gadioli Erba, G.Tagliaferri, Nuovo Cim. Riv., 6, 1 (1976).

11. K.K.Gudima and V.D.Toneev, JINR E4-9489, Dubna, 1976.

12. K.K.Gudima, S.G.Mashnik and V.D.Toneev, In "Calculations of Nuclear Structure and Nuclear Reactions", Shtiintsa, Kishinev, 1977, p. 12.

13. V.Weisskopf, Phys.Rev., 52, 295 (1937).

14. N.Bohr, J.A.Wheeler, Phys.Rev., 56, 426 (1939).

15. I.Dostrovsky, Z.Fraenkel, G.Friedlander. Phys.Rev., 110, 683 (1959).

16. I.Dostrovsky, H.Gauvin, M.Lefort, Phys.Rev., 169, 836 (1965).

17. V.S.Barashenkov, F.G.Gereghi, A.S.Iljinov, V.D.Toneev, Nucl.Phys., A206, 131 (1973).

18. H.L.Anderson, E.P.Hincks, C.S.Johnson, K.Rey, A.M.Segar, Phys.Rev., 133, B392 (1964).

19. G.Campos Venuti, G.Fronterotta, G.Mathiae, Nuovo Cim., 34, 1446 (1964).

20. P.M.Hattersley, H.Muirhead, J.N.Woulds, Nucl.Phys., 67, 309 (1965).

21. R.Hartman, H.P.Isaak, R.Engfer, E.A.Hermes, H.S.Pruys, W.Dey, H.J. Pfeiffer, U.Sennhauser, H.K.Walter, J.Morgenstern, Nucl.Phys., A308, 345 (1978).

22. N.S.Mukhopadhyay, J.Hadermann, K.Junker. SIN preprint PR-77-017, 1977; Nucl.Phys., A319, 448 (1979).

23. Yu.G.Budyashov, B.G.Zinov, A.D.Konin, N.B.Rabin, A.M.Chatrchyan. JETF, 62, 21 (1972).

24. P.J.Castleberry, L.Coulson, R.C.Minehart, K.O.H.Ziock, Phys.Lett., 348, 57 (1971).

25. J.C.Comiso, F.Meyer, F.Schleputz, K.O.H.Ziock. Phys.Rev.Lett., 35, 13 (1975).

26. W.Dey, R.Engfer, H.Guyer, R.Hartman, E.A.Hermes, H.P.Issak, J.Mongestren, H.Muller, H.S.Pruys, W.Reichart, H.K.Walter. Helv. Phys.Acta, 49, 778 (1976).

27. H.S.Pruys, R.Engfer, R.Hartman, E.A.Hermes, H.P.Issak, H.J.Preiffer, U.Sennhauser, H.K.Walter. Conf. on Nuclear Reaction Mechanism, Varenna, 1977.

28. G.Mechtersheimer, G.Buchee, U.Klein, W.Kluge, H.Matthay, D.Munchmeyer, A.Moline, Phys.Lett., 73B, 115 (1978).

29. F.W.Schleputz, J.C.Comiso, T.C.Meyer, K.O.H.Ziock. Phys.Rev., 19C, 135 (1979).

30. H.S.Pruys, R.Engfer, R.Hartman, U.Sennhauser, H.J.Pfeiffer, H.K.Walter, J.Morgenstern, A.Wyttenbach, E.Gadioli, E.Gadioli Erba. Nucl. Phys., A316, 365 (1979).

31. A.S.Iljinov, V.I.Nazaruk, S.G.Mashnik, S.E.Chigrinov. Short Communications in Physics, FIAN, 1, 14 (1979).

32. B.Betak, P.Oblozinsky, Contribution presented at the V Int. Symp. on Interactions of Fast Neutrons with Nuclei Gausing (GDR), 1975.

33. F.E.Bertrand, R.W.Peelle, Phys.Rev., 8C, 1045 (1973).

34. Z.Lewandowski, E.Loeffler, R.Wagner, H.H.Mueller, W.Reichart, P.Schober, H.Jasicek, P.Reihs. Phys.Lett., 80B, 350 (1979).

35. J.R.Wu, C.C.Chang, H.D.Holmgren, Phys.Rev., 19C, 698 (1979).

36. S.Ozaki, E.Weinstein, G.Glasse, E.Loh, L.Neimala, A.Wattenberg, Phys.Rev.Lett., 4, 533 (1960).

37. M.E.Nordberg, K.F.Kinsey, R.L.Burman, Phys.Rev., 165, 1096 (1968).

38. D.M.Lee, R.C.Minehart, S.E.Sobotka, K.O.Ziock, Nucl.Phys., A197, 106 (1972).

39. D.M.Lee, R.C.Minehart, S.E.Sobotka, K.O.Ziock, Nucl.Phys., A182, 20 (1972).

40. H.K.Walter, W.Dey, H.J.Pfeiffer, U.Sennhauser, R.Engfer, R.Hartmann, E.A.Hermes, H.P.Issak, H.Muller, H.S.Pruys, F.Schleputz, J.Morgenstern, A.Wyttenbach, Helv. Phys. Acta, 50, 561 (1977).

41. B.Bassalleck, H.D.Engelhardt, M.Furic, E.L.Haase, W.D.Klotz, C.W.Lewis, F.Ttakeutchi, H.Uiirich, Phys.Lett., 65B, 128 (1976).

42. R.Bassalleck, W.D.Klotz, F.Takeuchi, H.Ullrich, M.Furik, Phys.Rev., 16C, 1526 (1977).

43. B.Bassalleck, W.D.Klotz, F.Takeuchi, H.Ullrich, M.Furik, Z.Phys., A286, 401 (1978).

44. T.T.Sugihara, W.F.Libby, Phys.Rev., 88, 587 (1952).

45. A.Turkevich, J.B.Niday, Phys.Rev., 90, 342 (1953).

46. A.Turkevich, Si Chang Fung, Phys.Rev., 92, 521 (1953).

47. L.Winsberg, Phys.Rev., 95, 198 (1954).

48. H.Ullrich, E.T.Bbosvhitz, H.D.Engelhardt, C.W.Lewis, Phys.Rev.Lett., 33, 433 (1974).

49. B.Coupat et al. Phys.Lett., 55B, 286 (1975).

50. V.S.Butsev, Ya.Vandlik, Ts.Vylov, Zh.Ganzorik, L.Tumnerova, N.G.Zaitseva, S.M.Polikanov, O.V.Savchenko, D.Chultem, JINR P6-8541, Dubna, 1975.

51. V.S.Butsev, D.Chultem, Yu.K.Gavrilov, Dz.Ganzoring, V.Presperin, JINR E15-10210, Dubna, 1976.

52. H.D.Engelhardt, C.WLewis, H.Ullrich, Nucl.Phys., A298, 480 (1976).

53. V.M.Abazov, V.S.Butsev, Yu.K.Gavrilov, V.Presperin, D.Chultem, JINR P15-10684, Dubna, 1977.

54. V.S.Butsev, L.Vasharoshg, Zh.Ganzorig, Yu.V.Norseev, D.Chultem, JINR P15-10665, Dubna, 1977.

55. H.S.Pruys, R.Hartman, R.Engfer, U.Sennhauser, W.Dey, H.J.Pfeiffer, H.K.Walter, Helv. Phys.Acta. 50, 199 (1977).

56. P.Ebersold, B.Aas, W.Dey, R.Eichler, H.J.Leisi, W.W.Sapp, H.K.Walter, Phys.Lett., 58B, 428 (1977).

57. Y.Cassagnou, H.E.Jackson, J.J.Julien, R.Legrain, L.Roussel, S.Barbarino, A.Palmeri, Phys.Rev., 16C, 741 (1977).

58. R.Beetz, F.W.N. de Boer, J.K.Panman, J.Konijn, P.Pavlopoulos, G.Tibell, K.Zicutas, I.Bergstrom, K.Fransson, G.Backenstoss, L.Tauscher, P.Blum, R.Guigas, H.Koch, H.Poth, L.M.Simons, Z.Physik, A286, 215 (1978).

59. C.E.Stronach, H.S.Plendl, H.O.Funsten, W.J.Kossler, B.J.Lieb, V.G.Lind, Nucl.Phys., A308, 290 (1978).

60. V.S.Butsev, Zh.Ganzorig, S.M.Poilikanov, D.Chultem. Proc. 25 Conference on Nuclear Spectroscopy and Nuclear Structure, Leningrad, 1975.

61. V.M.Abazov, S.R.Avramov, V.S.Butsev, E.P.Cherevatenko, D.Chultem, W.D.Fromm, Dz.Ganzoring, Yu.K.Gavrilov, S.M.Polikanov, JINR E15-9659, Dubna, 1976.

62. V.S.Butsev, D.Chultem, E.P.Cherevatenko, Yu.K.Gavrilov, S.M.Polikanov, JINR E15-9825, Dubna, 1976.

63. V.S.Butsev, JINR P45-10847, Dubna, 1977.

64. M.P.Locher, F.Myhrer, Helv.Phys.Acta, 49, 123 (1976).

65. S.S.Gershtein, Usp. Fiz. Nauk. 124, 455 (1978).

66. A.S.Iljinov, V.I.Nazaruk, Proc. All-Union Seminar on the Program of Experiments on Meson Factory, Zvenigorod, 1977.

67. W.J.Kossler, H.O.Funsten, B.A.MacDonald, W.F.Lankford, Phys.Rev., 14C, 1551 (1971).

68. C.W.Lewis, H.Ulrich, H.D.Engelhardt, E.T.Boschitz, Phys.Lett., 47B, 339 (1973).

69. C.E.Stronach, W.J.Kossler, H.O.Funsten, W.F.Lankford, B.J.Leib, Phys.Rev., 15C, 984 (1977).

70. W.John, W.F.Fry, Phys.Rev., 91, 1234 (1953).

71. N.A.Perfilov, O.V.Lozhkin. V.P.Shamov. JETF 28, 655 (1955).

72. G.E.Belovitsky, T.A.Romanova, L.V.Sukhov, I.M.Frank, JETF, 29, 537 (1955).

73. N.A.Perfilov, N.S.Ivanova, JETF 29, 551 (1955).

74. Yu.A.Batusov, Zh.Ganzorig, O.Otgonsuren, D.Chultem. JINR P15-8917, Dubna, 1975.

75. U.Moser, A.Fluckiger, B.Hahn, E.Hugentobler, H.Kaspar, G.Viertel, R.P.Redwine (to be published); See ref. /22/.

76. E.Gadioli, E.Gadioli Erba, A.Moroni, Z.Phys., A288, 39 (1978).

77. L.S.Moretto, S.G.Thompson, J.Routti, R.G.Gatti, Phys.Lett., 38B, 471 (1972).

78. A.V.Ignatyuk, M.G.Itkis, V.N.Okolovich, G.N.Smirenkin, A.S.Tishin, Yad.Fiz., 21, 1185 (1975).

79. A.S.Iljinov, E.A.Cherepanov, E.E.Chigrinov, Z.Phys., A287, 37 (1978).

80. W.D.Myers, W.J.Swiatecki, Ark.Fys., 36, 343 (1977).

81. J.R.Nix, Nucl.Phys., A130, 241 (1969).

82. H.C.Pauli, J.Ledergerber. Nucl.Phys., A175, 545 (1971).

83. H.J.Krappe, J.R.Nix, Proc. 3-rd IAEA Symp. on the Physics and Chemistry of Fission, 1973. Paper IAEA-SM-174/12, Vol. 1.

84. J.R.Nix, E.Sassi, Nucl.Phys., 81, 1 (1966).

85. N.T.Porile, B.J.Dropesky, R.A.Williams, Phys.Rev., 18C, 2231 (1978).

86. A.S.Iljinov, E.A.Cherepanov, Preprint INR 11-0064, Moscow, 1977.

87. R.W.Haase,,Ann.Phys., 68, 377 (1971).

88. R.W.Hasse, W.Stocker, Phys.Lett., 44B, 26 (1973).

89. G.Sauer, H.Chandra, U.Mosel, Nucl.Phys., A264, 221 (1976).

90. B.Bassalleck, H.D.Engelhardt, W.D.Klotz, F.Takeutchi, H.Ullrich, M.Furic, CERN preprint, Geneva, 1978.

91. V.S.Butsev, D.Chultem, Phys.Lett., 67B, 33 (1977).

92. V.M.Abazov, V.S.Butsev, M.Milanov, N.Nenov, D.Chultem, JINR D6-11574, Dubna, 1978.

93. I.S.Shapiro, V.M.Kolybasov, JETF 44, 270 (1963).

94. T.I.Kopaleishvili, Particles and Nuclei, Atomizdat, 2, 439 (1971).

95. R.Bizzarri,E.DiCapua, U.Dore, G.Gialanella, P.Guidoni, I.Laakso, Nuovo Cim., 33, 1497 (1964).

96. M.M.Block, T.Kikuchi, D.Koetke, J.Koperman, C.R.Sun, R. Walker, C.Culligan, V.L.Telegdi, R.Winston, Phys.Rev.Lett., 11, 301 (1963).